



Vrije Universiteit Brussel

Faculty of Engineering  
Department of Mechanical Engineering

# Study and Design of an Actuated Below-Knee Prosthesis

---

Graduation thesis submitted in partial fulfillment of the  
requirements for the degree of Master in Applied Sciences and Engineering:  
Electro-Mechanical Engineering, Mechanical Engineering

**Joost Geeroms**

---

Promotor: Prof. dr. ir. Dirk Lefebber  
Copromotor: Prof. dr. ir. Bram Vanderborght  
Advisor: Pierre Cherelle

JUNE 2011





Vrije Universiteit Brussel

Faculteit Ingenieurswetenschappen  
Vakgroep Toegepaste Mechanica

# Studie en Ontwerp van een Geactueerde Onderbeenprothese

Proefschrift ingediend met het oog op het behalen  
van de graad van Master in de Ingenieurswetenschappen:  
Werktuigkunde-Elektrotechniek, Werktuigbouwkunde

**Joost Geeroms**

Promotor: Prof. dr. ir. Dirk Lefebber  
Copromotor: Prof. dr. ir. Bram Vanderborght  
Begeleider: Pierre Cherelle

JUNI 2011



## Acknowledgements

This was a beautiful project to work on, not only challenging and enriching, but it is also satisfying to know that the work done, even if it's only a very small part of the puzzle, can eventually help people walk with less effort.

I would like to thank my promotor professor Lefeber and copromotor professor Vanderborght for enabling me make my contribution to this project. Many thanks to Pierre who helped me throughout the whole process of making this thesis work, from the first simulation to the last written part. Also, every other professor, assistant, technician, doctor, PhD student or fellow student in the department who helped me when I had questions on whatever subject, it has been greatly appreciated.

The rest of the gratitude I have left goes to the people that read my thesis or got involved in any other way, and to my girlfriend, who often insisted that I made backups of my work, like she also did just before my laptop crashed...

Joost Geeroms

## Abstract

Almost all of the transtibial prostheses, which are for below-knee amputations, that are available on the market are purely passive devices. They store energy in an elastic element during the beginning of a step and release it at the end in order to move the body forwards. The main problem with these prostheses is that only the energy that has been stored in the elastic element is used for the push-off, unlike for sound ankles where the muscles provide extra energy. There are a few prostheses who use active components for this energy input, but these are still in research phase.

The problem with transtibial prostheses that use a DC motor for this energy input is that this motor has to deliver the energy in a small period of time and thus requires high power. The objective of this thesis is to study the possibility of storing energy during an other part of the gait cycle and then releasing it when necessary. In this case the energy is stored in a spring using a motor with a relatively low rated power. The difficulty with this concept is that it requires a rather complicated mechanical system with different lever arms from which the position with respect to each other has to be lockable.

In this thesis first a simulation was made to get a first estimate of the required motor power and the properties of the other components. The goal of this simulation is to achieve a model that is able to provide the same characteristics as a sound ankle and that is ideally adaptable for different walking conditions.

The next step was to develop this first model, with a driving system and all of the other components present. This design was then to be further optimised to become as light and compact as possible, while being able to withstand the forces and torques that are exerted by the driving system and the body weight. These static and dynamic forces are examined in a stress analysis.

The result of this research is a prosthesis that can be described in short as: (for a person of 75 kg)

- A prosthesis mimicking the sound ankle behaviour, having an energy output that is equally high and that occurs at the right time.
- A prosthesis with a driving system consisting of a motor with a rated power of only 30 W, a gearhead and a ball screw mechanism.
- A system for which the properties can be changed by altering the pretensions of the springs and the motor operation.
- A total mass of the prosthesis of under 2 kg. The batteries are not included in this calculation.
- A compact design which is able to withstand all the acting forces.
- An energy consumption of 28.9 J per step.

## Samenvatting

Bijna alle beenprothesen die beschikbaar zijn in de handel zijn puur passieve apparaten. Deze slaan energie op in een elastisch element tijdens het eerste deel van een stap en laten deze vrij bij het einde zodat deze kan gebruikt worden om het lichaam voorwaarts te bewegen. Het belangrijkste probleem met deze prothesen is dat enkel de energie die in het elastisch element gestockeerd werd, gebruikt wordt voor de push-off. Dit is niet het geval bij een gezonde enkel, waar de spieren extra energie leveren. Er zijn enkele prothesen die actieve elementen gebruiken voor deze extra energie, maar deze zijn nog steeds in onderzoeksfase.

Het probleem met prothesen die een DC-motor gebruiken voor deze extra energie is dat de motor deze energie moet leveren in een kleine tijdsspanne en dat dus een hoog vermogen vereist is. Het doel van deze thesis is de mogelijkheid om energie te stockeren in een ander ogenblik van de stapcyclus en deze op het gepaste moment te laten vrijkomen. In dit geval wordt de energie opgeslaan in een veer door gebruik te maken van een motor met een relatief laag vermogen. De moeilijkheid in dit concept is dat er nood is aan een eerder ingewikkeld mechanisch systeem met verschillende hefboomsarmen van welke de positie ten opzichte van elkaar moet kunnen geblokkeerd worden.

In deze thesis werd eerst een simulatie gemaakt om een eerste schatting te krijgen van het nodige motorvermogen en de eigenschappen van de andere componenten. Het doel van deze simulatie is een model te verkrijgen dat in staat is hetzelfde gedrag als een gezonde enkel te vertonen en dat in het ideale geval aanpasbaar is voor verschillende stapcondities.

De volgende stap was dit eerste model te ontwikkelen, met een aandrijfsysteem en al de andere nodige componenten aanwezig. Dit design werd dan verder geoptimaliseerd om zo licht en compact mogelijk te zijn, terwijl het toch bestand moet blijven tegen de krachten en koppels die uitgeoefend worden door het aandrijfsysteem en het lichaamsgewicht. Deze statische en dynamische krachten werden bestudeerd door middel van een spanningsanalyse.

Het resultaat van dit onderzoek is een prothese die in het kort op de volgende manier beschreven kan worden: (voor een persoon van 75 kg)

- Een prothese die het gedrag van een gezonde enkel benaderd, met een energieoutput die even hoog is en op hetzelfde moment optreedt.
- Een prothese met een aandrijfsysteem dat bestaat uit een motor met een vermogen van slechts 30W, een gearhead en een ballscrewmechanisme.
- Een systeem waarvan de eigenschappen kunnen aangepast worden door de voorspanningen van de veren en de motoroperatie aan te passen.
- Een totale massa van minder dan 2 kg. De batterijen zijn niet meegenomen in deze berekening.
- Een compact ontwerp dat in staat is alle optredende krachten te weerstaan.
- Een energieverbruik van 28,5 J per stap.

## Résumé

Presque toutes les prothèses trans-tibial disponibles sur le marché sont des appareils passifs. Ces prothèses stockent de l'énergie dans un élément élastique pendant la première phase d'un pas et la relâchent ensuite pour propulser le corps. Le problème le plus important avec ces prothèses est que seule l'énergie qui a été stockée dans l'élément élastique est utilisée pour la propulsion. Dans le cas d'une cheville saine en revanche les muscles du mollet fournissent l'énergie supplémentaire. Certaines prothèses utilisent des composants actifs pour acquérir cette énergie, mais celles-ci sont encore en une phase de développement.

Les prothèses utilisant un moteur à courant continu pour cette énergie supplémentaire connaissent le problème suivant : ce moteur doit offrir cette énergie durant une courte période, et ce moteur doit être très puissant. L'objectif de ce mémoire est d'examiner si il est possible de stocker de l'énergie pendant une phase précise de la marche et de relâcher cette énergie pendant une autre phase. Dans le cas présent, l'énergie est stockée dans un ressort en utilisant un moteur de puissance raisonnable. La difficulté de ce concept est qu'un système mécanique assez compliqué est nécessaire, avec des bras de levier dont la position par rapport aux autres doit pouvoir être bloquée.

Tout d'abord, une simulation a été faite pour obtenir une estimation de la puissance nécessaire du moteur et des caractéristiques des autres composants. L'objectif de cette simulation est de développer un modèle capable de fournir les mêmes caractéristiques qu'une cheville saine et qui, dans le cas idéal, peut être adapté aux conditions de marche différentes.

Ensuite, ce premier modèle a été développé avec une système motorisé et la présence de tous les autres composants. Ce design a ensuite été optimisé pour le rendre le plus léger et le plus compact possible, et en même temps capable de résister aux forces et aux couples qui sont exercés par la motorisation et le poids corporel. Ces forces statiques et dynamiques sont examinées dans une analyse de résistance des matériaux.

Le résultat de cette recherche est une prothèse qui peut être décrite en bref comme: (pour une personne de 75 kg)

- Une prothèse capable d'imiter le comportement d'une cheville saine, avec une production d'énergie qui est aussi élevée et qui a lieu au moment propice.
- Une motorisation d'une puissance de seulement 30W, un réducteur et un mécanisme de vis à billes.
- Une système dont lequel les caractéristiques peuvent être adaptés par varier la précontrainte des ressorts et l'opération du moteur
- Une masse totale de la prothèse de moins que 2 kg. Les batteries non-incluses.
- Un design compact et capable de résister à toutes les forces agissantes.
- Une consommation d'énergie de 28.9 J par pas.

## Abbreviations

DF: DorsiFlexion

E: Energy

F: Force

FF: Foot Flat

HO: Heel Off

IC: Initial Contact

MDF: Maximum DorsiFlexion

P: Power

PF: PlantarFlexion

T: Torque

TO: Toe Off

TT: TransTibial

$\omega$ : Rotational speed

# Contents

<b>1</b>	<b>Biomechanics of human walking</b>	<b>9</b>
1.1	Basics . . . . .	9
1.1.1	Gait cycle terminology . . . . .	9
1.1.2	Key phases . . . . .	11
1.2	Ankle characteristics . . . . .	15
1.2.1	Ankle terminology . . . . .	15
1.2.2	Ankle behaviour . . . . .	15
<b>2</b>	<b>Transtibial prostheses: State of the art</b>	<b>19</b>
2.1	Definition . . . . .	19
2.2	Conventional feet . . . . .	19
2.3	Energy storing and returning feet . . . . .	20
2.4	Active prostheses . . . . .	23
2.4.1	Prostheses with artificial muscles . . . . .	24
2.4.2	Electrically powered prostheses . . . . .	25
<b>3</b>	<b>Design of an actuated below-knee prosthesis</b>	<b>28</b>
3.1	Development of the concept . . . . .	28
3.1.1	Previous concepts . . . . .	28
3.1.2	First concept . . . . .	30
3.1.3	Optimization of concept . . . . .	32
3.2	Step by step explanation of final concept . . . . .	32
3.2.1	Phase 1 . . . . .	32
3.2.2	Phase 2 . . . . .	34
3.2.3	Unlocking . . . . .	35
3.2.4	Phase 3 . . . . .	36
3.2.5	Swing phase . . . . .	37
3.3	Adaptability . . . . .	38
3.3.1	Changing the spring pretension . . . . .	38
3.3.2	Changing the motor operation . . . . .	39
3.4	Choice of components . . . . .	41
3.4.1	Driving system . . . . .	41
3.4.2	Motor . . . . .	41
3.4.3	Springs . . . . .	46
3.4.4	Locking mechanism . . . . .	49
3.4.5	Conclusions . . . . .	51
3.5	Control and electronics . . . . .	52
3.5.1	Sensors . . . . .	52
3.5.2	Sensors for operation . . . . .	52
3.5.3	Motor control . . . . .	55
3.5.4	Motor autonomy . . . . .	58
3.6	Prosthesis design . . . . .	60
3.6.1	Initial design phase . . . . .	61
3.6.2	Final design . . . . .	62
<b>4</b>	<b>General conclusions and future work</b>	<b>83</b>
	<b>References</b>	<b>85</b>



# 1 Biomechanics of human walking

## 1.1 Basics

### 1.1.1 Gait cycle terminology

The gait cycle can be defined as the time interval between two consecutive occurrences of the same recurring event during walking. This event can for example be the moment the right foot touches the ground. The gait cycle can be subdivided into two periods for each leg: the stance and the swing period. The stance period is defined by the contact between the leg and the ground, and during the swing period there's no contact with the ground. The stance is about 60% of the total cycle. This indicates that there's an overlap between the stance periods of the 2 legs, and during 20% of the gait both legs have ground contact [12].

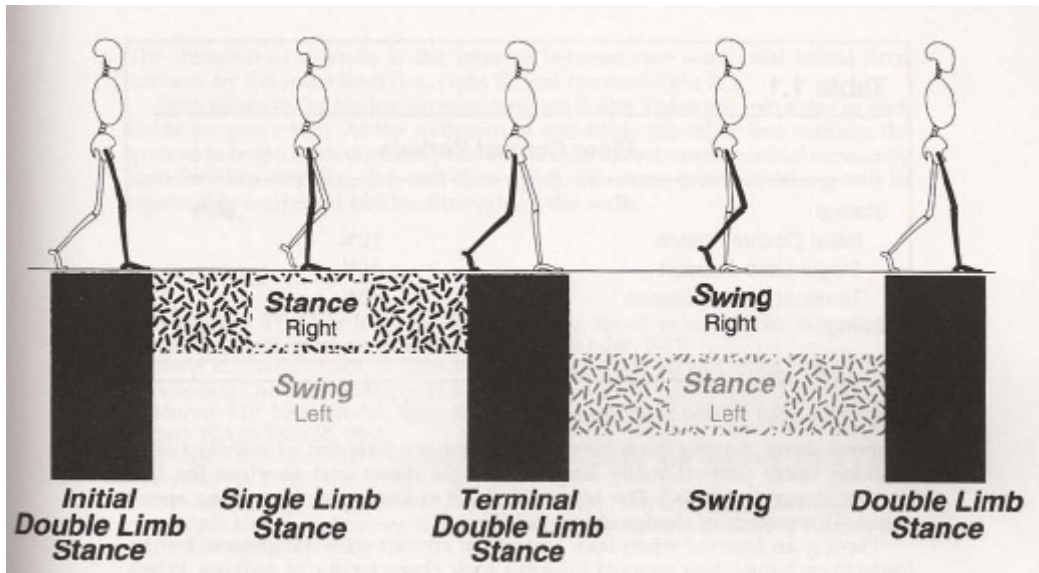


Figure 1.1: Overview of the human gait cycle.

There are three reference planes that are used when talking about human anatomy. The sagittal plane, the frontal plane and the transverse plane are depicted in Fig.1.2. For most of this work, all of the movements and forces are projected onto the sagittal plane.

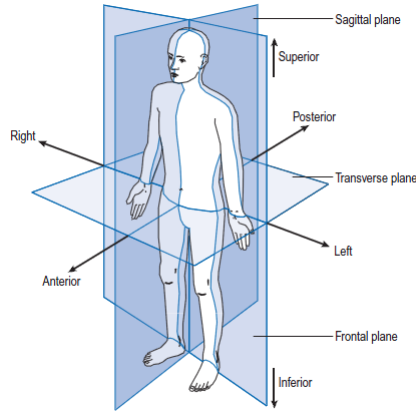


Figure 1.2: The anatomical position and orientation with the three reference planes.

There are two important terms to describe distances in relation to human gait: step and stride. The step length is defined as the distance between two consecutive ground contacts of one of the feet. The stride on the other hand is the distance between two consecutive ground contacts of one foot and the other one. This means that the stride is the sum of the left step and the right step, and in an ideal gait pattern these two are the same. The determination of these distances are necessary in order to be able to define walking speeds afterwards.

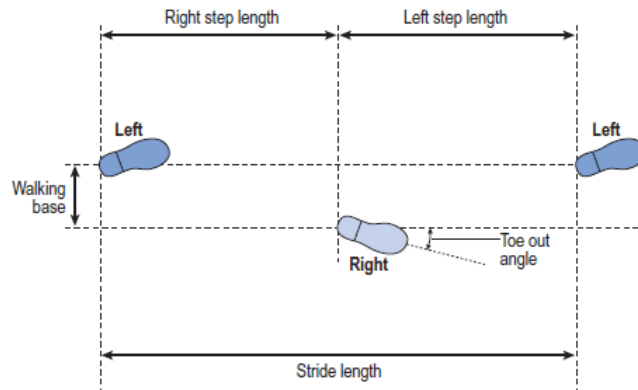


Figure 1.3: Stance and stride.

Similarly to the distance, there are a few important terms to describe time and speeds in relation to the human gait. The number of steps a person takes during a certain amount of time is his cadence. The problem with this variable is that since the common unit is steps per minute, it measures half cycles per unit of time, which is not considered to be scientifically acceptable.

Another reason is that for people with pathological gait, left step and right step is not necessarily equally large. Better is to use the cycle time or stride time, which is the time it takes the person to move two steps, or one stride. It's relation to the cadence is:

$$cycle\ time\ (s) = \frac{120}{cadence\ (steps/minute)} \quad (1.1)$$

From this cycle time the walking speed can be calculated if the length of one stride is divided by it:

$$speed\ (m/s) = \frac{stride\ length\ (m)}{cycle\ time\ (s)} \quad (1.2)$$

The forces occurring during the gait cycle can be described in different ways. A first method is to draw the ground reaction forces on certain times at a fixed interval during the stance phase. This leads to a so-called butterfly diagram, where the horizontal and vertical forces are plotted versus time, either in seconds or in percentage of gait. As can be noticed in Fig. 1.4, the ground reaction force vectors only exist during the stance phase, since there is no ground contact during the swing phase [19].

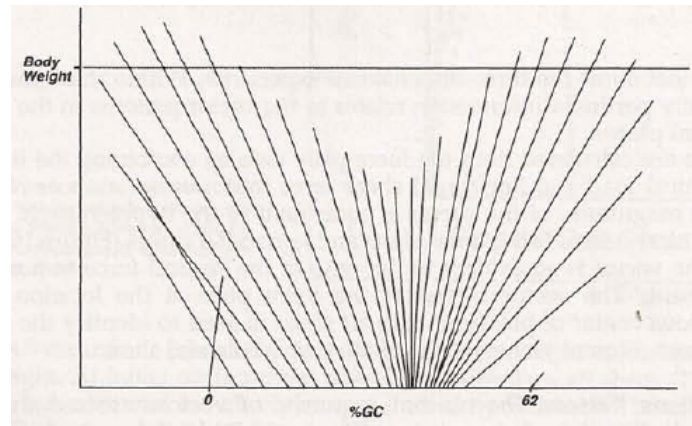


Figure 1.4: Ground reaction force vectors during the gait cycle. 5 % of gait cycle intervals.

### 1.1.2 Key phases

The gait cycle is mostly divided in more detail by describing 8 key phases, 5 during stance and 3 during swing. During stance the heel strike, loading response, midstance, terminal stance and

pre-swing occur, during swing acceleration, midswing and deceleration.

1. Heel strike: This is the phase that starts with the Initial Contact (IC), where the foot makes contact with the ground. Its the begin of the stance and the foot is prepared to roll over the heel. This takes place during the first 2% of the gait cycle.

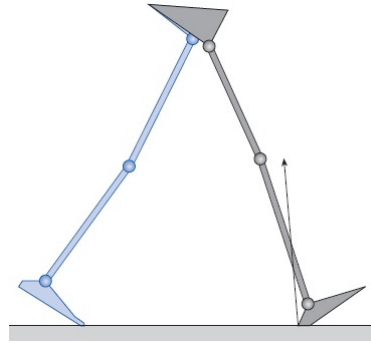


Figure 1.5: Initial Contact. The arrow represents the ground reaction force.

2. Loading response: After rolling over the heel, the rest of the foot touches the ground which is called Foot Flat (FF). The ground reaction forces increase and rotate backwards as the weight of the body is transferred from the other leg and the heel carries most of that weight. The force is about 120% of the body weight at this point. The body moves downward to its lowest point of the whole cycle. The phase ends when the other leg begins its swing and the double support period is ended. This takes place during the first 10% of the gait cycle.

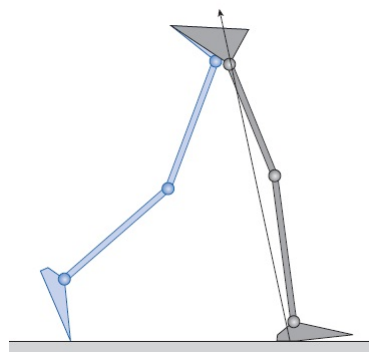


Figure 1.6: Loading response.

3. Mid Stance: The whole foot keeps its contact with the ground while the other leg is moved forward. The ground reaction forces rotate forward as the body rotates around the ankle joint. The body climbs to it's highest point of the gait cycle while it's weight is distributed over the whole foot. The phase ends when the two legs are adjacent and the ground reaction force is pointing upward.

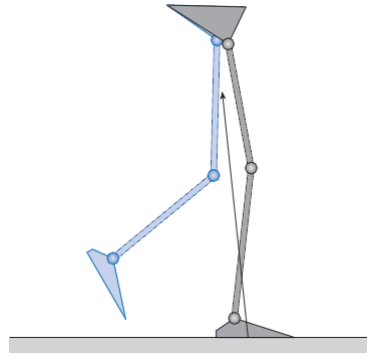


Figure 1.7: Mid Stance.

4. Terminal stance: The weight of the body is transferred to the front of the foot as the center of gravity of the body lies in front of the ankle. The ground reaction force rotates further forward and it grows as push-off is generated: the whole body is pushed forward by the limb. This phase ends at Heel Off (HO), where the contact between the heel and the ground is ended.

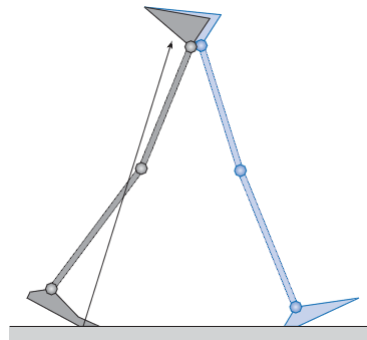


Figure 1.8: The initial contact of the other foot. This is the event that separates terminal stance from pre-swing.

5. Pre-swing: This phase starts with the IC of the other leg and the end of the single limb

support phase. The leg and foot now rotate around the toe joint. The ground reaction force starts to drop since the weight is transferred to the other leg (weight release), while it continues to rotate forward. This phase as well as the stance phase end at Toe Off (TO), when the ground contact of the toe is ended.

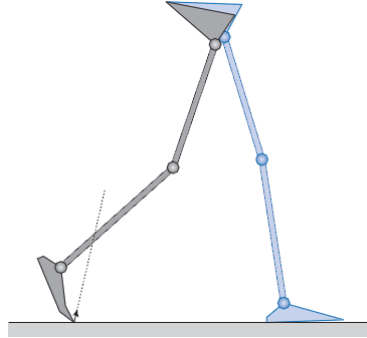


Figure 1.9: Toe off. This indicates the end of the pre-swing phase.

6. Initial swing or acceleration: The foot is lifted from the ground and the leg is accelerated forward while the weight of the body is carried by the other leg.
7. Midswing: The leg is adjacent to the other leg while it continues to swing forward.

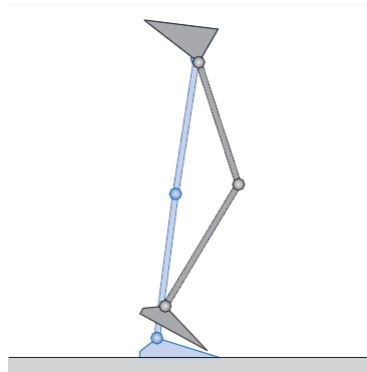


Figure 1.10: The center of the swing phase. The two feet are next to each other.

8. Terminal swing or deceleration: The limb is slowed down and prepared to make ground contact. This phase ends with IC. [12,19]

## 1.2 Ankle characteristics

### 1.2.1 Ankle terminology

Since the subject in this thesis is the development of a TransTibial (TT) prosthesis, and the purpose of this device is to mimick the behaviour of a sound ankle during the gait cycle, the terminology and characteristics of the ankle will be explained in further detail. The definition of the reference planes is the same as defined before, with the frontal, sagittal and transverse plane. There are different terms to describe rotations about the ankle in the different planes. In the sagittal plane, the rotation which causes the toes to move upwards, closer to the leg, is called DorsiFlexion (DF). The rotation in the other direction, so downward for the toes, is called PlantarFlexion (PF). These rotations are used the most frequently since mostly kinematics are studied in this plane. Rotations in the frontal plane are called inversion when the foot rotates towards the other foot and eversion when it moves away from it. For rotations in the transverse plane the terms are adduction for a rotation towards the other foot and abduction for the opposite. [17]

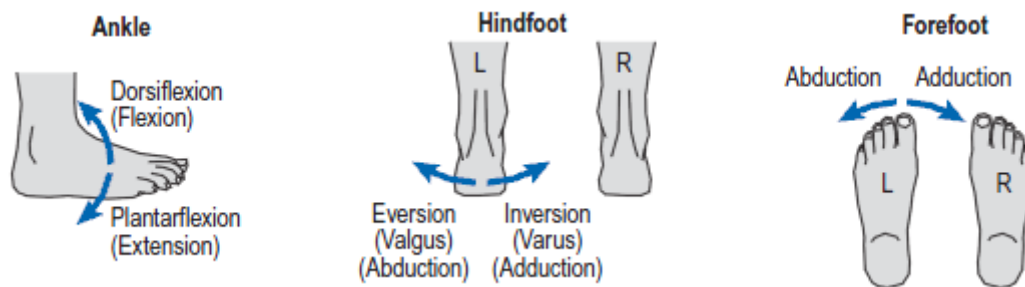


Figure 1.11: Ankle rotations in the different reference planes. Left: sagittal plane, middle: frontal plane, right: transverse plane

### 1.2.2 Ankle behaviour

In the past, biomechanical studies have been performed on the ankle and from those, the ankle behaviour was described using different characteristics. For this thesis work, the studies of Winter have been used [21]. The angle of the leg and the torque around the ankle joint were measured during the gait cycle. The important events that are reviewed before are indicated on the figures: IC, FF and TO. HO is not depicted on the figures, since there's another term that

is more suitable when talking about the ankle behaviour, called Maximum Dorsiflexion (MDF). This is the moment where the angle of the leg is maximal. Also, the phases that occur during the gait cycle are called differently in this case, based on the direction of rotation around the ankle joint. The first phase between IC and FF is referred to as controlled plantarflexion, the phase between FF and MDF is called controlled DF and the phase from MDF to TO is called powered PF. “Controlled” indicates that the muscles of the leg and foot are used to absorb the energy during these phases, “powered” means that additional energy from the muscles is used to provide push-off.

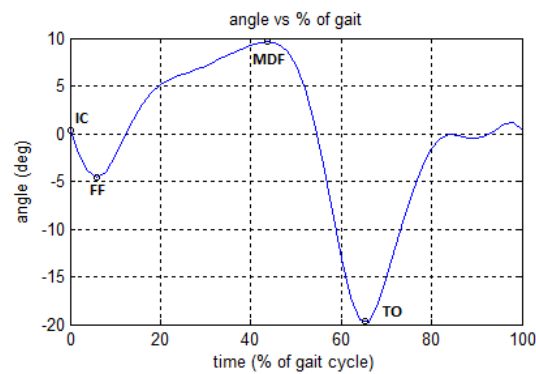


Figure 1.12: Angle versus % of gait cycle

At IC, the angle of the leg is around  $0^\circ$ . Until the end of the loading phase, there is a plantarflexing rotation to around  $-5^\circ$ . After this, there's a dorsiflexing rotation during mid stance and terminal stance until the leg is at approximately  $10^\circ$ . After this, the push off occurs in the pre-swing phase and the leg angle decreases to  $-20^\circ$  in a second plantarflexing rotation. During the initial swing there is another dorsiflexing rotation, after which the angle remains  $0^\circ$  for the rest of the swing phase.



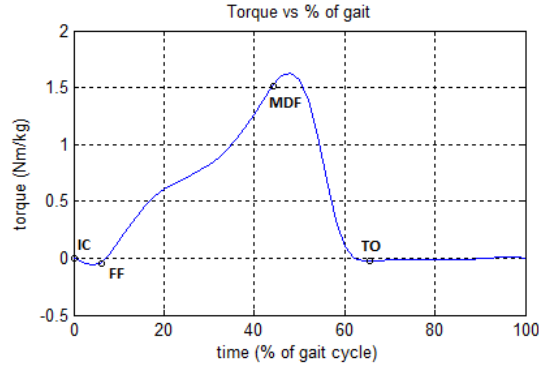


Figure 1.13: Torque versus % of gait cycle

At IC, the torque is 0 Nm, after which there will be a small dorsiflexor torque during the loading phase. During mid stance, the torque will increase and become a plantarflexor torque. This will continue until MDF, and then the torque will increase even more after this until it reaches about 1.7 Nm per kg of body weight. During pre-swing, the torque drops to reach 0 Nm at TO.

A graph that is frequently used in literature is the combination of the two previous ones (Fig. 1.14), where the torque around the ankle joint is plotted against the angle of the ankle.

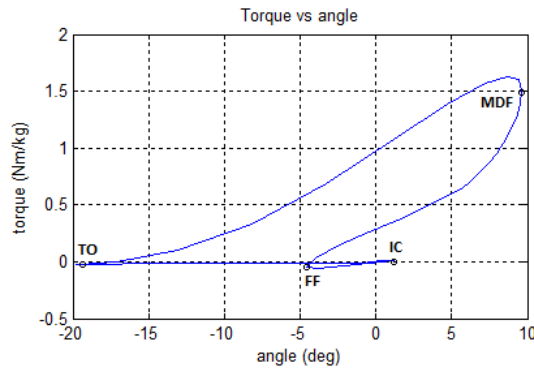


Figure 1.14: Torque versus angle

The reason why this graph is considered useful by a lot of researchers is that it shows an other important useful parameter: the ankle stiffness. This is especially important in prosthetics, where attempts are made to mimic the ankle behaviour by using elastic springs. These are specifically used to create the same ankle stiffness as for a healthy ankle. This will be further explained later

in this work.

Another variable that is interesting to look at and that can be calculated from the ankle angle and torque is the ankle power.

$$P = T \times \dot{\alpha} \quad (1.3)$$

In which the ankle P is the ankle power, T is the torque around the ankle and  $\dot{\alpha}$  is the ankle angular speed. The angular speed is calculated by computing the time derivative of the ankle angle.

$$\dot{\alpha} = \frac{d\alpha}{dt} \quad (1.4)$$

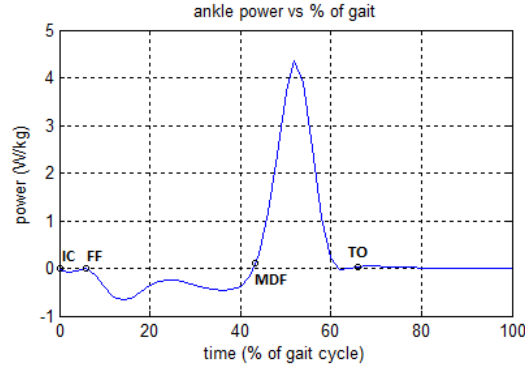


Figure 1.15: Ankle power versus % of gait cycle

The graph shows that the work done between IC and MDF is negative, which means energy is stored here, but after MDF there is a rapid increase in power, up to more than 4 Watts per kilogram body weight. This is the power used to provide the push off. The energy used by the ankle during one gait cycle can be calculated by computing the integral of the power, which gives a value of just over 0.22 J/kg body weight, which is about 16.6 J for an average person of 75 kg.

$$E = \int P dt = 16.6 J \quad (1.5)$$

## 2 Transtibial prostheses: State of the art

### 2.1 Definition

According to Black's Medical Dictionary [16], a prosthesis is “an artificial replacement of a missing or malfunctioning body part”. The prostheses looked upon in this work are devices which replace body parts after amputation, the “severance of a limb, or part of a limb, from the rest of the body”. The term transtibial implies that the limb in this case is the lower leg, and that the amputation happened between the knee and the ankle. The tibia is the largest bone in the lower leg, connecting to the thigh bone at the knee joint and to the ankle joint at its other end.

### 2.2 Conventional feet

Until the '80s the focus in the design of prosthetic feet was on trying to restore basic walking and enabling the amputee to fulfill basic tasks. Examples of this can be found back to the ancient times where wood, bronze or iron were used to make substitutes for lost limbs. A well known example of this kind of prostheses is the simple wooden leg that was used during the dark ages. The prostheses and materials used slowly evolved until the so-called “conventional feet”, which were still very basic but from these prostheses onward things like weight of the prosthesis and amputee comfort became more important. The SACH-foot, which stands for Solid Ankle-Cushion Heel [1,8], is the most common of these conventional feet. It has been developed at the University of California in the 1950s and has long been by far the most prescribed prosthesis in the USA. As the name says, the prosthesis has a soft, compressible heel that first of all damps the impact on the ground but also provides so called “pseudo-plantarflexion” after IC. It's not really PF because the ankle does not change in angle but it simulates the effect. The “Solid Ankle” refers to the fact that the ankle joint does not rotate, and the core of the prosthesis is a rigid wooden keel. Though this prosthesis is an improvement with respect to earlier prostheses and it has been used a lot, it still limits the amputee in his movements and actions. Despite this, the prosthesis is still popular, mainly in developing countries. The reasons for this are its low cost and weight and high reliability thanks to the lack of rotating mechanical parts.



Figure 2.1: The SACH-foot (left and middle) and the uni-axial foot (right)

A second popular prosthesis was the uni-axial foot [8]. This prosthesis does have a single rotating joint in the ankle. There are two bumpers at both sides of the ankle joint which limit the foot in its rotation. The first bumper limits the PF movement of the foot and also provides a DF torque from heel strike to foot flat. The second bumper limits the DF movement and provides a PF torque after foot flat. This prosthesis is heavier than the SACH-foot and because of the rotating mechanical parts it needs maintenance more often. When the temporal distribution of the stride for both prostheses is compared, it can be seen that the SACH-foot has more time between heel-strike and foot-flat, which provides a roll-over which is more comfortable. The uni-axial foot on the other hand provides more stability because of its early foot flat. Also, this type of prosthesis is more suitable for uneven terrain because the ankle can turn in the sagittal plane. Studies have shown that for most amputees, the prosthesis they are used to wearing is considered the best of both [8].

### 2.3 Energy storing and returning feet

Driven by the higher demands and needs of amputees, like for example jumping, running and practicing sports, the prosthetic feet were improved over time. An important group of these amputees, although not the largest group, were veterans who lost limbs in war, since a lot of the research is and was funded by the military. The Seattle foot [1,9], developed in 1981 at the VAMC (Veteran Affairs Medical Center) in Seattle, Washington, was one of the first prosthetic foot which stored energy in one part of the gait cycle and returned it in another part. Hereby the push-off is improved and thus moving forward is made easier for the amputee. The Seattle foot stores the energy in its flexible keel and releases it after MDF. There are many prostheses with designs that were released in the years after the Seattle foot, all of them using a flexible

keel to store the energy. Some examples are given in Fig. 2.2.

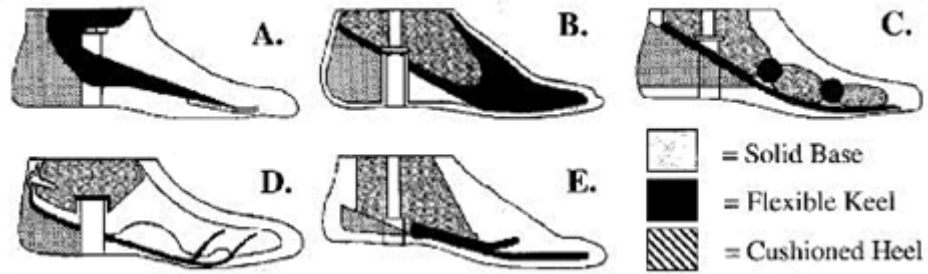


Figure 2.2: Early ESR prostheses. A: Seattle foot B: Dynamic foot C: STEN foot D: SAFE foot E: Carbon Copy foot.

Another prosthesis that was very popular, especially in developing countries because of its simple design and low cost is the Jaipur foot. It has been developed in the city with the same name in India. The Jaipur foot was first developed in the 1960s as a cheap prosthesis for victims of landmines in India, but it evolved into a prosthesis that could compete with the other early ESR prostheses. The prosthesis has a wooden ankle and the foot itself consists of a combination of different types of rubber. Tests measuring ground reaction forces comparing the Jaipur, Seattle and SACH-feet showed that the Jaipur foot was experienced to be the closest to the gait of a healthy limb [1].

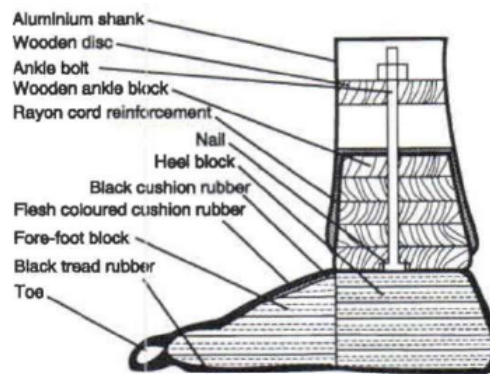


Figure 2.3: The Jaipur Foot

Thanks to a better knowledge and understanding of the human gait and biomechanics, the development of new (composite) materials and the evolution of Computer Aided Design (CAD) and Manufacturing (CAM), new types of ESR prostheses were developed. One of the first types

was the Flex-foot, which consisted of a flexible carbon-fiber composite material. Its biomechanical properties were better than those of the early ESR-feet and a lot of similar prostheses were built in response. Whereas early ESR-feet tried to make parts of a prosthetic foot store energy, these devices were designed to store as much energy as possible in the whole prosthesis. The use of carbon-fiber material allowed the energy losses and the weight of the prostheses to be reduced, which gave them a significant advantage to earlier designs.



Figure 2.4: ESR feet. 1: Ossür Flex-footModular III, 2: Ossür Flex-foot Variflex, 3: Otto Bock Springlite Foot, 4: Ossur Flex-foot Talux

Rather than storing energy during stance and then releasing it in late stance, it is also possible to use the weight of the body on initial contact to store energy and release this later in the stance to provide a better push-off. The Controlled Energy Storing and Returning foot (CESR foot), developed at the university of Michigan and the University of Delft is based on this principle. This prosthetic foot has a rotating joint in the middle of the foot which locks after heel strike. During heel strike, a spring in the heel is compressed and the energy in this spring is released during push-off when the rotating joint unlocks [6].

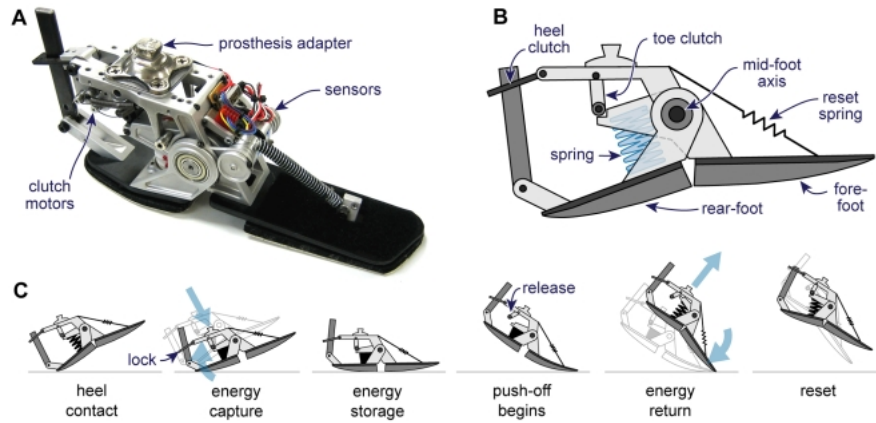


Figure 2.5: CESR foot

As seen in Winter's angle-torque characteristic of able-bodied gait cycle, the ankle rotates about 15 degrees during controlled DF while it stores energy. After this, it rotates about 30 degrees while releasing this energy. If a prosthesis should imitate this behavior, two different ankle stiffnesses would be needed for those phases. At the Vrije Universiteit Brussel, a TT prosthesis has been developed called the Ankle-Mimicking Prosthetic foot (AMPfoot) [17]. This device consists of a spring and a planetary gearbox, and its working principle is based on a change in equilibrium position of the spring. Using a planetary gearbox and locking mechanisms allows to have a different transmission ratio between the rotating leg and the lever arm that extends the spring during loading and unloading. In order to store enough energy during the loading phase, a high torque has to be achieved at MDF, which leads to a severe drop in torque after unlocking. Tests showed that this made it hard to walk with the prosthesis.

## 2.4 Active prostheses

All of the prostheses described so far use only the energy provided by the amputee himself to mimic the behavior of a sound ankle. There is also the possibility to insert energy into the system by using an external source of energy. The type of source can differ, but so far two types have been investigated in various universities: pressurised gas used to power artificial muscles and electrical energy to power motors.

### 2.4.1 Prostheses with artificial muscles

Since transtibial (TT) amputees lack propulsive force because they don't have their ankle musculature anymore, the university of Washington [7] investigated if they could make artificial muscles which have the same behavior as biological muscles. A prosthesis was developed which used artificial muscles to replace the triceps surae and the Achilles tendon, two muscles in the lower leg. The goal of the prosthesis was to achieve the same torque and range of rotation as a sound ankle, as described by Winter [21]: a peak torque of 110 Nm for a person of 80 kg and 30° of rotation. Test results showed that the relation between the force, velocity and length measured with the artificial muscles were a good first order approximation of the mathematically predicted relation based on static and dynamic properties of biological muscles.

At the Vrije Universiteit Brussel, a TT prosthesis using artificial muscles was developed [17]. This prosthesis used Pleated Pneumatic Artificial Muscles (PPAMs), which, thanks to the use of its pleated membrane, does not experience material stretching when inflated [18]. Test results showed that the extended push-off was experienced by the amputee.

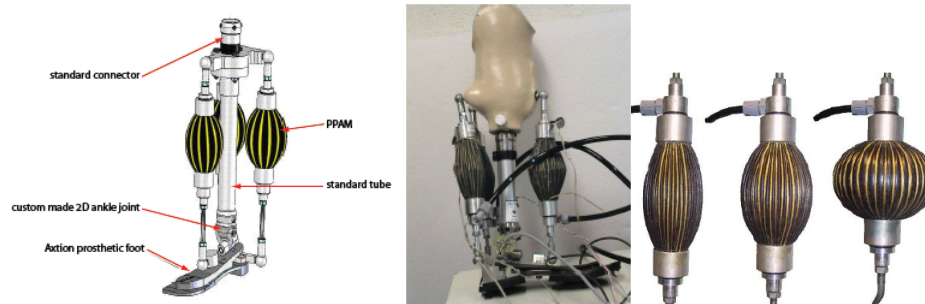


Figure 2.6: Prosthesis with PPAMs developed at the Vrije Universiteit Brussel (left and middle), 2nd generation PPAMs in three different contraction stages (right).

In comparison to electric actuators like motors, artificial muscles have a large power over weight ratio and they are safer because they are inherently compliant. Also, stiffness and power can be regulated by altering the pressure in the muscles, which makes it very easy to adjust the prostheses to the needs of the amputee. The artificial muscles however have got disadvantages too, like the need for pressurised gas which limits the application to rehabilitation processes.



### 2.4.2 Electrically powered prostheses

Prostheses powered by means of electrical energy are mostly still in a research phase, just like prostheses with artificial muscles. A single commercially available active prosthesis is the Proprio Foot, developed by Össur. However, the motor and the inputted energy is not used to store additional energy for improved push-off, but rather to adjust the properties of the prosthesis to different types of terrain.



Figure 2.7: Össur Proprio foot. Image adapted from [www.ossur.com](http://www.ossur.com)

The rest of the existing electrically powered prostheses are prototypes developed by universities. One of them is the MIT Powered Foot Prosthesis [2,3]. Its working principle is based on a high-power actuator with series elasticity. This so called Series-Elastic Actuator (SEA) [13,14,20] consists of a high-power DC motor with mechanical transmission and a spring in series. The motor adds energy to the system and changes the joint stiffness and damping by stretching and shortening the series spring. A second spring was placed in parallel to store part of the energy for angles larger than  $0^\circ$ . This way, the load on the SEA is reduced when the torques are the highest, around MDF.

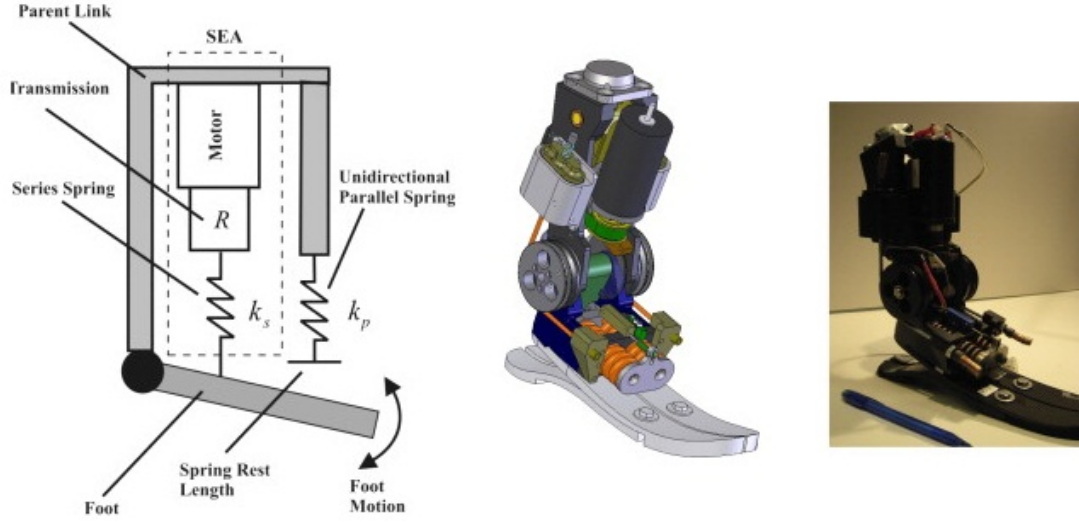


Figure 2.8: The MIT Powered Foot Prosthesis. Left: schematic of the prosthesis, middle: CAD drawings, right: the actual prototype.

Another prototype is developed at the Arizona State University in a multi-phased project. SPARKy (Spring Ankle with Regenerative Kinetics) uses a Robotic Tendon actuator, which is a light actuator with a low power motor and a screw mechanism which changes the position of helical springs during the gait cycle [10]. The actuator stores kinetic energy within the spring and adds motor energy. By doing this, the peak motor power required to provide the necessary energy for the push-off is 77 W (for SPARKy 1, the first phase of the SPARKy project), whereas a direct drive system would require a 250 W motor. A motor of this size would weigh about 6.6 kg, but the Robotic Tendon for SPARKy 1 weighs 7 times less. Further research and improvements lead to SPARKy 2, with an even lighter motor, and SPARKy 3, which allows movement in both the coronal and sagittal planes to further improve the mobility of the amputees [4].

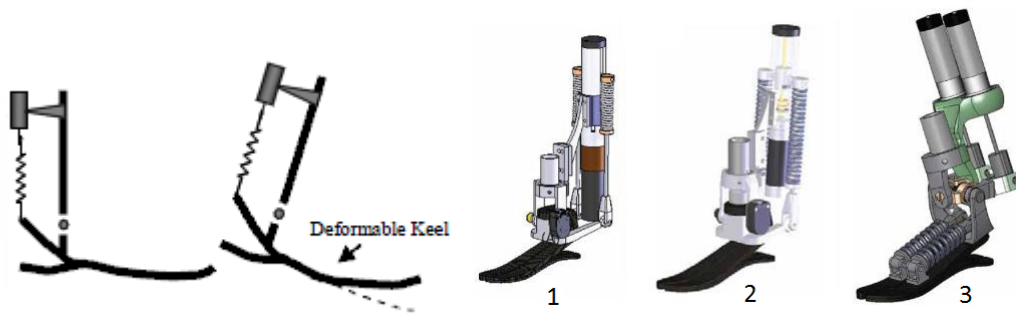


Figure 2.9: Schematic of the SPARKy prosthesis (left), the three different SPARKy designs (right)

## 3 Design of an actuated below-knee prosthesis

### 3.1 Development of the concept

#### 3.1.1 Previous concepts

The objective of this thesis is to design an actuated prosthesis that could replace the function of the ankle for people with a TT amputation. To this purpose, a DC motor is used to provide additional energy. In order to make sure the prosthesis' behaviour is the same as that of a sound ankle, gait cycle data of an average able-bodied person [21] is used and the device is designed to match this as good as possible.

If the ankle behaviour was to be simulated using only linear spring characteristics and no active components, three different spring stiffnesses would be necessary in order to get a reasonable approximation. During controlled PF, there is a change in torque of 4 Nm for a change of angle of  $5^\circ$  for a person of 75 kg. From this we can calculate the ankle stiffness:

$$c = \frac{\Delta T}{\Delta \alpha} = \frac{4Nm}{5^\circ} = 0.8Nm/^\circ \quad (3.1)$$

During controlled DF on the other hand, there is a change in torque of 135 Nm for a change in angle of  $15^\circ$ :

$$c = \frac{135Nm}{15^\circ} = 9Nm/^\circ \quad (3.2)$$

During powered PF there is a change in torque of 130 Nm for a change in angle of  $30^\circ$ :

$$c = \frac{130Nm}{30^\circ} = 4.33Nm/^\circ \quad (3.3)$$

A prosthesis can be imagined that consists only of three springs, for example linear springs attached to the leg by using a lever arm or with linear torsion springs. If we compare this to the

sound ankle data in Fig. 3.1, one can see that this is not a very good approximation, especially for controlled DF and powered PF. A solution for this would be to use springs with a non-linear characteristic. An other problem with this design is that it would require 2 locking mechanisms that can connect or disconnect the springs from the leg. The change from  $1 \text{ Nm}/^\circ$  to  $9 \text{ Nm}/^\circ$  can easily be done by adding a spring parallel to the first one, but going from  $9 \text{ Nm}/^\circ$  to  $4.33 \text{ Nm}/^\circ$  would require the addition of a spring in series. This would first of all cause a torque drop and because of that a significant loss of energy. The torque ankle-characteristic in Fig. 3.1 would never look like the red graph but rather like the green one.

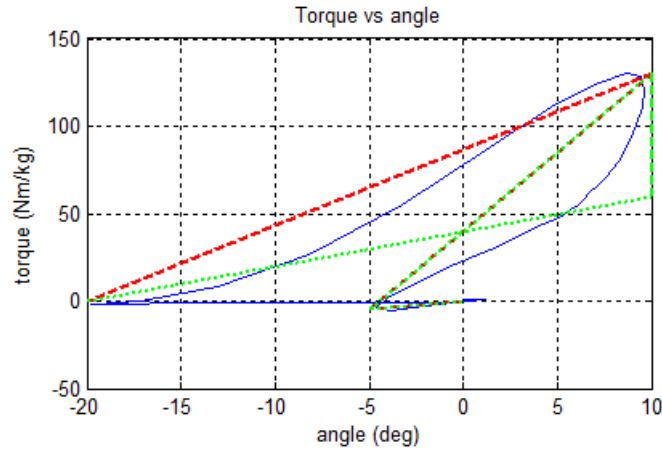


Figure 3.1: Passive concept of TT prosthesis. In blue the data of a sound ankle, in red the three different spring constants and in green a realistic simulation of a system with three springs.

Changing the stiffness of the ankle is possible using an active component like a motor or pneumatic actuators. The problem with pneumatic actuators is that it requires a pressurized vessel nearby, as has been explained before. A dc motor can be used in a Series Elastic Actuator (SEA) [13,14,20], so with a transmission and an elastic spring in series connected to the leg. The motor has to work from before MDF to TO, extending the spring and by that adding energy and changing the ankle stiffness. If a prosthesis would be designed based on this principle, it would still require two different springs, one to provide the plantarflexor torque between IC and FF, and one with another stiffness for during controlled dorsiflection. The prosthesis would be able to approach the sound ankle's behaviour from FF to MDF. The amount of energy that is added to the gait by a sound ankle from MDF to TO can be calculated by computing the integer of

the power vs gait cycle graph (Fig. 1.15) between these values.

$$E = \int P dt \quad (3.4)$$

This value of about 17 J for a person of 75 kg is the amount of energy that has to be added by the motor and the time between these two points is about 20 % of the gait cycle or 0,2 s. From this, an approximation of the motor power that would be necessary can be calculated.

$$P_{motor} = \frac{17J}{0.2s} = 85W \quad (3.5)$$

If motor and transmission efficiencies are included this means a motor with a rated power of over 100 W is necessary [15].

It is possible to reduce this power, and with that the weight of the motor and the reduction. The proposed solution, that will be further elaborated in this work, is to use a second locking mechanism that allows a motor to store energy in a spring over a longer time-span. If for example the motor is able to operate from IC to TO, with release of the energy at MDF, this would increase the operating time from 0.2s to 0.6s, which decreases the power with the same ratio.

$$P_{motor} = \frac{17J}{0.6s} = 28.3W \quad (3.6)$$

### 3.1.2 First concept

A first version of the concept is shown in Fig. 3.2. It has 3 different springs, connected to the ankle joint through lever arms. The other components are a motor and a locking mechanism that locks the large lever arm.

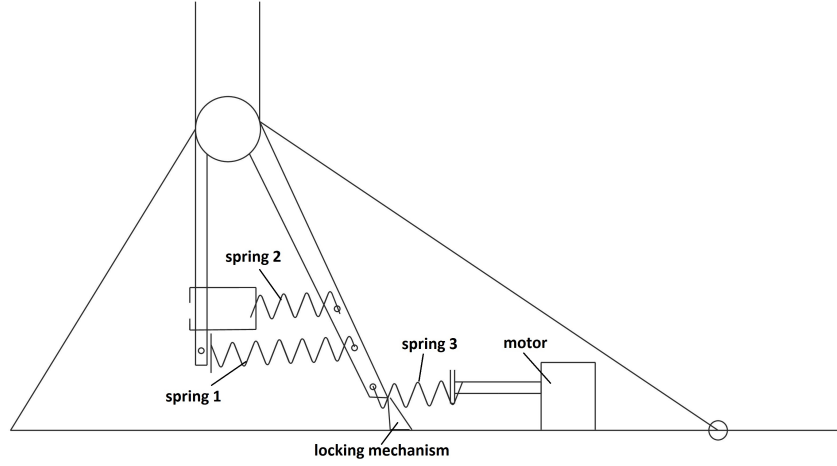


Figure 3.2: A first concept of the TT prosthesis.

The working principle is as described above: spring 1 provides a dorsiflexor torque between after IC and returns the torque to 0 Nm afterwards, spring 2 provides a plantarflexor torque until MDF, after which the locking mechanism unlocks and springs 2 and 3 in series provide the plantarflexor torque until TO. The torque-angle characteristic of this system is shown in Fig. 3.3.

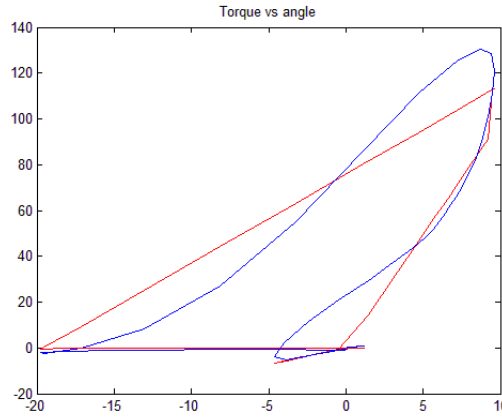


Figure 3.3: torque-angle characteristic of a sound ankle in blue and the initial prosthesis concept in red. Torques in Nm and angles in  $^{\circ}$ .

Although the same trends can be noticed between the two curves, the approximation is still not very good.

### 3.1.3 Optimization of concept

Several aspects of this initial concept can be improved:

- In order to be able to adjust the prosthesis' behaviour to the need of the amputee it is important to have the ability to modify the prosthesis characteristics. Since it is impossible to change the spring's stiffnesses without replacing the springs, the pretension should be changeable. In previous concept changing the pretension would imply a change in orientation of the lever arms too, so to avoid this the lever arms should be aligned with the springs in between them.
- At FF, the stiffness should change right away instead of going back to 0 Nm first before the second spring starts to be stretched out. In order to be able to do this, a second locking mechanism can be added. Spring 2 can be connected to another lever arm from which the orientation can be unlocked from the orientation of the leg. By doing this, the spring is not affected between IC and FF, but it is from FF onwards.

## 3.2 Step by step explanation of final concept

The concept will now be described step by step. The whole gait cycle will be covered, starting from IC. The system is drawn in Fig. 3.4. It has 3 springs that are connected to the ankle joint by lever arms. The other components are a motor and locking mechanisms. A simulation is made of the prosthesis, using the angles of a sound ankle as input and calculating the ankle torques by using the spring constants and pretensions.

### 3.2.1 Phase 1

At IC the angle of the leg is  $0^\circ$ , and all of the lever arms are aligned to each other under an ankle of  $30^\circ$  compared to the leg. The first lever arm is attached to the leg under a fixed angle, the second and third are connected to the leg through a bearing. The third lever arm is attached to the foot structure through a locking mechanism. The motor is extending a spring that is connected to this locked lever arm. Between IC and FF, the leg rotates to  $-5^\circ$  and so does lever arm 1, extending spring 1 to provide a dorsiflexor torque. Lever arms 2 and 3 remain at their initial position.



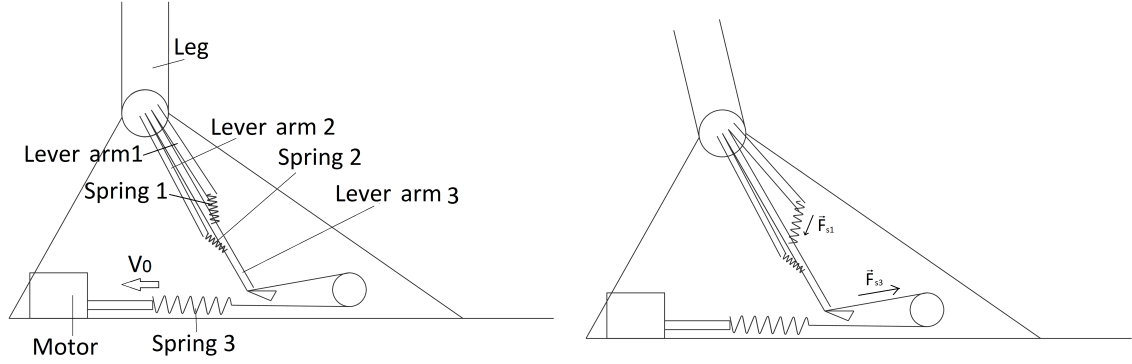


Figure 3.4: Foot at initial contact (left) and foot flat (right).

In order to know the ankle torque during this phase, we have to calculate the extension of the spring. The extension is, with the same notations as in Fig. 3.5(left) :

$$\Delta l = |\overline{DC}| - |\overline{DB}|$$

The force on the lever arm and the torque can be calculated from this:

$$\overline{T} = \overline{F} \times \overline{AC} = \Delta l \cdot k \cdot \overline{1_{CD}} \times \overline{AC} \quad (3.7)$$

Where  $k$  is the spring constant,  $T$  is the torque around the ankle,  $\Delta l$  is the spring extension.  $\overline{AC}$  and  $\overline{1_{CD}}$  are defined in Fig. 3.5.

For a choice of spring constant the torques can be calculated in the MATLAB simulation. The graph of the ankle torque versus the angle for the first phase is shown in Fig. 3.5.

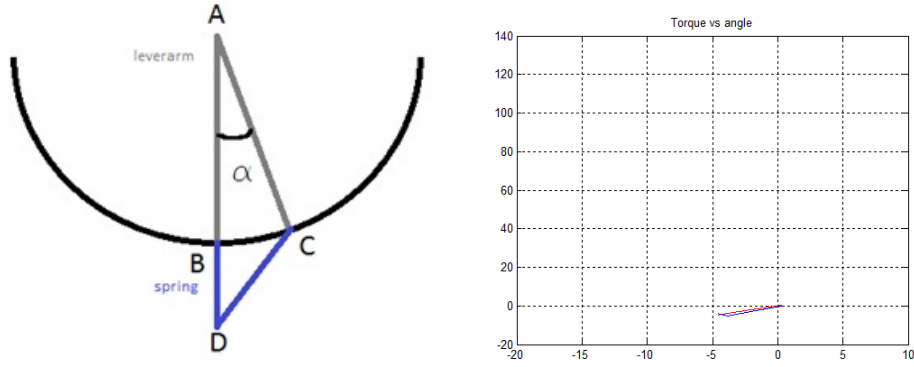


Figure 3.5: Schematic of spring extension (left), torque-angle characteristic of a sound ankle in blue and the prosthesis in red (right). Torques in Nm and angles in  $^{\circ}$ .

### 3.2.2 Phase 2

At FF, the locking mechanism between lever arm 2 and the leg locks and both lever arm 1 and lever arm 2 are attached to the leg. Between the two lever arms there is an angle of  $5^{\circ}$  due to the locking mechanism and this will remain like this until it unlocks. The leg rotates from  $-5^{\circ}$  to  $10^{\circ}$  and this rotation extends springs 1 and 2, which generate a plantarflexor torque until MDF. The calculation of the extension and the torque are the same as in the first phase but for the 2 springs. The resulting torque is the sum of the two calculated torques, which can be seen in Fig. 3.6. Throughout this phase, the motor keeps extending spring 3, which has no effect on the ankle torque because of the locking on lever arm 3.

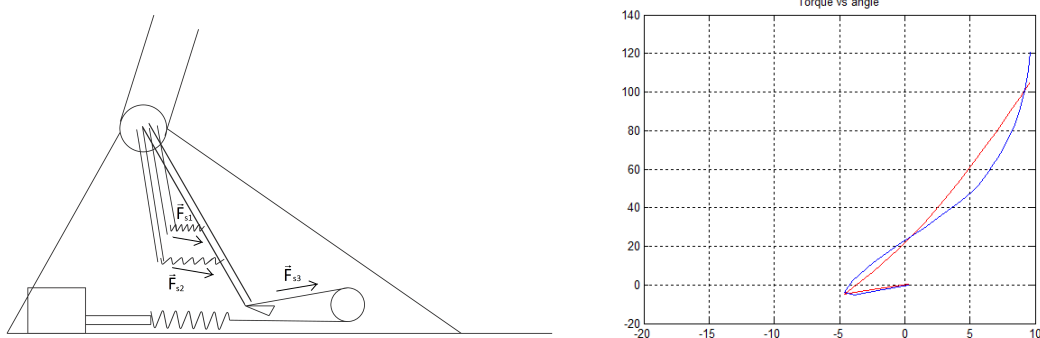


Figure 3.6: Foot at MDF (left), torque-angle characteristic of a sound ankle in blue and the prosthesis in red (right). Torques in Nm and angles in  $^{\circ}$ .

### 3.2.3 Unlocking

At MDF, the locking mechanism that prevents the third lever arm to rotate counterclockwise unlocks and the energy stored in spring 3 by the motor is released. Since the function of the motor is to introduce a rise in torque at MDF, the torque generated by the elongation of spring 3 on the time of unlocking has to be higher than the one generated by the elongation of springs 1 and 2. If this is the case, the third lever arm will rotate counterclockwise to a new equilibrium position as can be seen in Fig. 3.7.

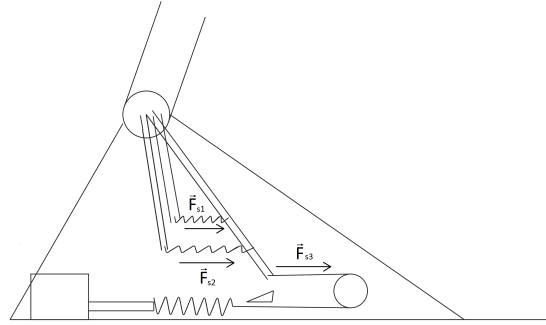


Figure 3.7: Foot at MDF after unlocking

In order to know the resultant torque, the equilibrium position of lever arm 3 has to be calculated. The schematic which is used to do this and the resulting torque are shown in Fig. 3.8

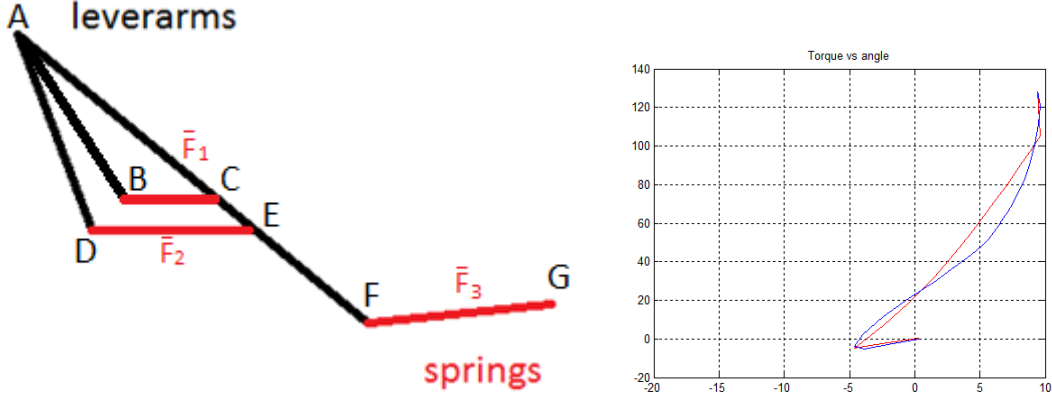


Figure 3.8: Schematic for calculation of equilibrium position (left), torque-angle characteristic of a sound ankle in blue and the prosthesis in red (right). Torques in Nm and angles in  $^{\circ}$ .

$$M_3 = |\overline{AF} \times \overline{F}_3| = M_{1+2} = |\overline{AE} \times \overline{F}_2| + |\overline{AC} \times \overline{F}_1| \quad (3.8)$$

Where  $M_3$  is the torque exerted by spring 3 around point A (being the ankle joint) and  $M_{1+2}$  is the torque exerted by springs 1 and 2 around point A, all with notations as in Fig. 3.8.

The unknown variable in this equation is the angle of the lever arm, so the direction of  $\overline{AF}$ ,  $\overline{AE}$  and  $\overline{AC}$ . This equation can be solved iteratively in MATLAB by using the “fsolve” function. With this function the difference between the two torques is set to zero by changing the angle between the lever arms. Once this angle is known the extension of the spring, the resulting force and the torque on the leg can be calculated in the same way as for phase 1 and 2:

$$M_2 = |\overline{AD} \times \overline{F}_2| \quad (3.9)$$

### 3.2.4 Phase 3

After the unlocking the assisted PF starts, where all the energy that has been stored in the springs, both by the controlled DF and the motor, is used for the PF. The ankle torque will

decrease until it reaches 0 Nm. The ankle torque can be calculated for all different angles by using the same method and MATLAB function as during unlocking. The motor can create an extra extension of spring 3 during this phase. By doing this, the resting position of the system of connected springs is changed. The goal of this is to achieve the torque of 0 Nm at an angle of  $-20^\circ$ , just like for a sound ankle.

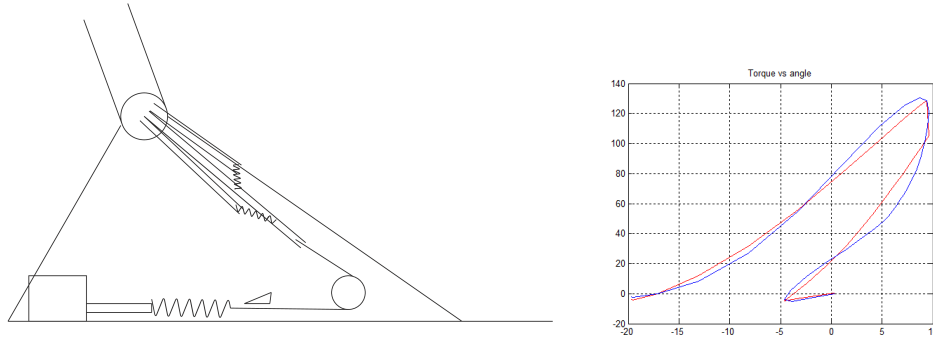


Figure 3.9: Foot at TO (left), torque-angle characteristic of a sound ankle in blue and the prosthesis in red (right). Torques in Nm and angles in  $^\circ$ .

### 3.2.5 Swing phase

When the ground contact is broken at TO, the locking mechanism that locks lever arm 2 will unlock and the motor will reverse it's sense of rotation to push spring 3 back. Lever arms 1, 2 and 3 will be pulled back to their initial position by a recall spring with a low spring constant, so that lever arm 3 can be locked again and the motor can restart extending spring 3 at IC. The small recall spring should not influence the prosthesis characteristics significantly

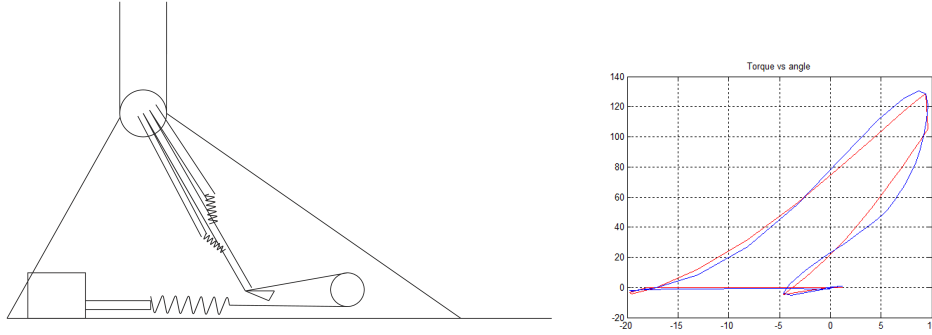


Figure 3.10: Foot during swing phase after locking of lever arm 3 (left), torque-angle characteristic of a sound ankle in blue and the prosthesis in red (right).

### 3.3 Adaptability

The ability to change the performance and the characteristics of the prosthesis without having to change the components would be an asset. The springs are placed in such a way that the pretensions can be changed and the motor operating speed can also be varied. In this section a few simple experiments will indicate that changing these variables, the prosthesis can be adjusted to the personal needs of an amputee.

#### 3.3.1 Changing the spring pretension

The spring that is connecting the small lever arm and the large lever arm is simulated with different values of the pretension. The result is shown in Fig. 3.12. For higher pretensions, the amount of stored energy rises as well as the torque on the ankle joint. This is logical, since a higher pretension causes a higher ankle stiffness. Lower pretensions cause a lower ankle stiffness.

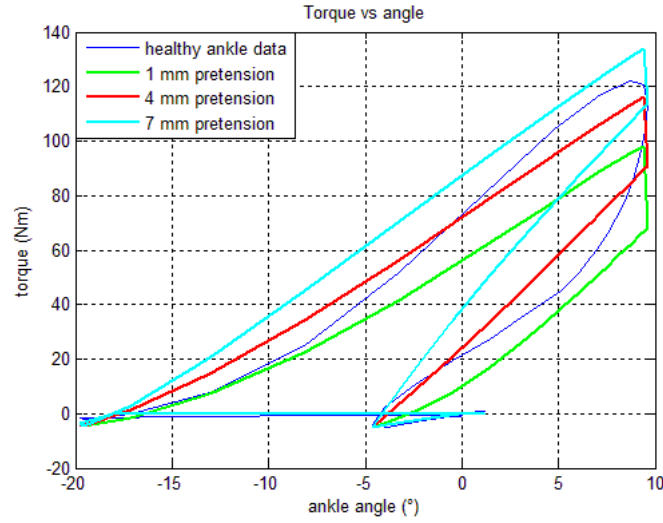


Figure 3.11: Torque-angle characteristic for three different pretensions of the spring providing the plantarflexor torque after FF. The blue line is the torque-angle characteristic of a healthy ankle for a person of 75 kg.

### 3.3.2 Changing the motor operation

The prosthesis is simulated for different motor operating speeds during the stance phase. First the rotating speed from IC to MDF is varied, as is shown in Fig. 3.12. Higher rotational speeds provide higher torque jumps at MDF. This is of course because more energy is stored in the spring that is connected to the motor.

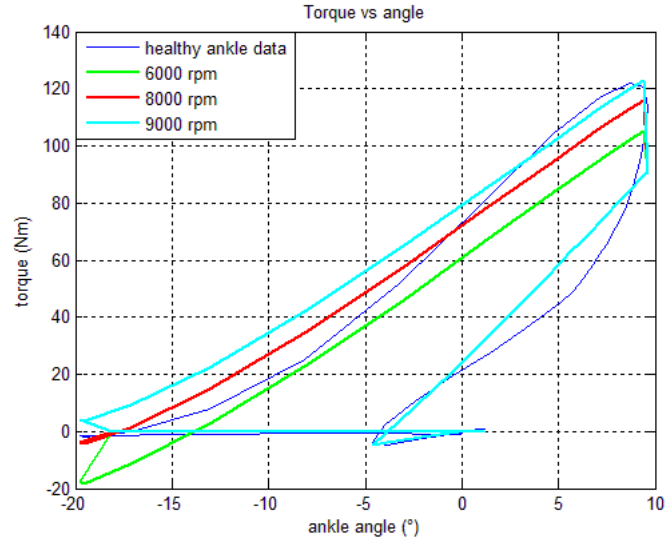


Figure 3.12: Torque-angle characteristic for three different motor rotational speeds between IC and MDF. The blue line is the torque-angle characteristic of a healthy angle for a person of 75 kg.

The prosthesis is also simulated for different motor rotational speeds between MDF and TO. The results in Fig. 3.13 show a different ankle stiffness for the assisted PF phase.

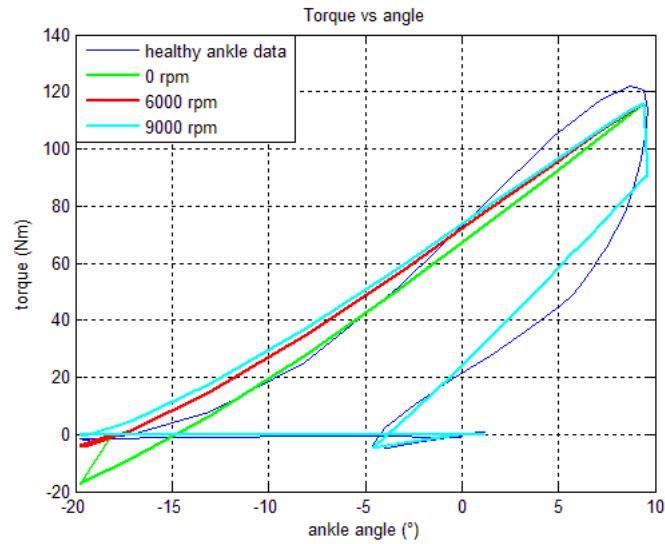


Figure 3.13: Torque-angle characteristic for three different motor rotational speeds between MDF and TO. The blue line is the torque-angle characteristic of a healthy angle for a person of 75 kg.



## 3.4 Choice of components

### 3.4.1 Driving system

Previously the driving system of the prosthesis was always referred to as “motor”, but the problem with a motor is that it provides a rotating movement whereas for the extension of the spring a longitudinal movement is needed. The driving system therefore will not only consist of a motor but also of a transmission which will transform the rotation to a translation.

### 3.4.2 Motor

The function of the motor is to provide the additional energy necessary for the push-off that cannot be stored in passive elements during the rest of the gait. The amount of energy that has to be added to the system has been calculated before (Eq. 3.4) and is about 17J. Since the motor has to provide this in 0.6 seconds, it's rated power should be about 30 Watts. We can also see this if we compare the power versus stride characteristic of a sound ankle and the same characteristic for a prosthesis with only passive elements.

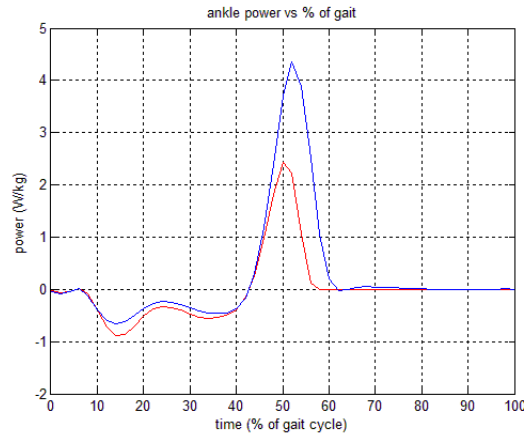


Figure 3.14: Ankle power versus % of gait of a sound ankle in blue and the prosthesis in red.

As could be expected, the integral of the red curve is equal to zero. In order to have the same energy output as a sound ankle, energy has to be added in an active manner.

Other than the rated power, it is important to know the demands of the system regarding rotational speed and torque if a motor has to be selected. These have to be calculated in the

simulation and the motor has to meet some requirements:

- The highest value of the calculated torque has to be lower than the peak torque, this means the torque cannot exceed the short-term operation region of the motor curve
- The RMS-value of the calculated torque cannot be higher the rated torque, this means this RMS value has to be in the continuous operation region of the motor curve.

In the calculation of these values however the transmission ratio is also needed. This ratio will be chosen so that the motor meets the requirements above, which are also visible in Fig. 3.15 where the operating region is shown.

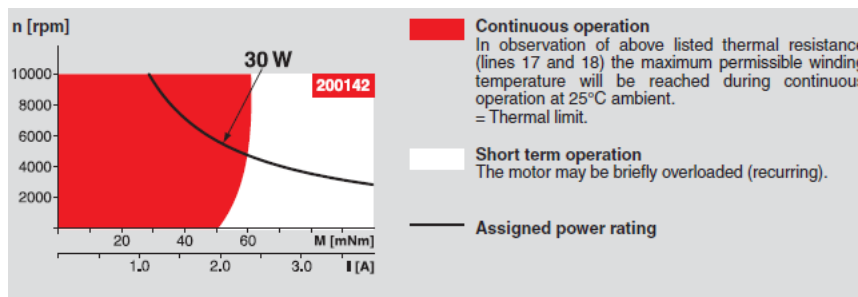


Figure 3.15: Operating region of a brushless motor (Maxon EC 45 flat).

Other requirements for the motor in this specific case are light weight and a compact design. The motor that has been selected is the Maxon EC 45 flat motor. The data sheet of the motor can be found in Appendix A.

**Transmission** The transmission has got two important functions: transforming the torque and rotational speed to make sure the motor requirements as explained in the previous paragraph can be met, and transforming the rotational movement into a translational movement.

The most apparent way to create a translation is by using a screw mechanism. With the spring connected to a nut on the screw and the motor turning the screw around, it is indeed possible to extend it. The problem with screw mechanisms is the high amount of friction and the low efficiency. A good alternative is a ball screw mechanism. It is the same principle as an ordinary screw mechanism, but it has small balls between the screw and the nut which reduce

the friction and improve the efficiency. Whereas the efficiency for ordinary screws is never higher than 70%, ball screws have efficiencies up to 95 %.



Figure 3.16: Ball screw mechanism. Image adapted from Bosch Rexroth website.

An important parameter for the selection of a ball screw mechanism is the lead, which defines the transmission ratio. Every time the screw makes one complete turn, this causes a translation of the nut over a length that is equal to the lead. The torque the motor has to provide can be calculated using this length if the force necessary to extend the spring is known.

$$T = \frac{F \times P}{2 \times \pi \times \eta} \quad (3.10)$$

Where  $T$  is the torque at the motor side in Nmm,  $F$  is the axial force on the nut in N,  $P$  is the lead in mm and  $\eta$  is the ball screw efficiency. For the axial force an estimate of 2400 N will be used. If a lead of 5mm is taken (based on maximum axial load of the ball screw) and an efficiency of 90% :

$$T = \frac{2400N \times 5mm}{2 \times \pi \times 0.9} = 2.12Nm \quad (3.11)$$

This is too high for the motor that was selected earlier. It is clear that an additional reduction is necessary in order to lower the torque on the motor. A possible solution is to lower the lead, but this would lower the maximum axial load on the ball screw and lower the efficiency. An other transmission has to be added to further reduce the torque on the motor. A gearbox placed

in between the motor and the ball screw mechanism can be used to do this. For the selected type of motor, different kinds of gearboxes are available. The most important ones are planetary gearheads and spur gearheads. Spur gearheads are the simplest kind of gearhead. They have two cogwheels per stage, with the first wheel of the first stage mounted on the motor shaft. The advantage of this type is that it is cheaper than the other types, with reasonably high efficiencies and low noise. The disadvantage is that it is suitable for low torques only, but since the continuous torque can go up to 2Nm this shouldn't be a problem. Planetary gearheads can transfer higher torques but are more expensive than spur gearheads. There are other types of gearheads that use different gears like worm gears, but they are less suitable for this application because they have a lower efficiency due to higher friction.

The transmission ratio that is necessary has to be calculated based on the torque at the gearhead output, the gearbox efficiency and the maximum torque at the motor output. In the case of a spur gearhead this gives:

$$T_{motor} = \frac{T_{gearbox} \times R}{\eta_{gearbox}} \rightarrow R = \frac{T_{motor} \times \eta_{gearbox}}{T_{gearbox}} = \frac{0.1Nm \times 0.76}{2.12Nm} = \frac{1}{27.89} \quad (3.12)$$

Where R is the reduction ratio of the gearbox and  $\eta$  in this case is the efficiency of a spur gearhead with 3 stages. The reduction ratio should be at least 1:28, which makes this gearhead with a reduction ratio of 1:32 suitable: the Maxon Spur Gearhead GS 45 A with 3 stages.

In case of a planetary gearhead the same calculation can be done:

$$R = \frac{0.1Nm \times 0.81}{2.12Nm} = \frac{1}{26.17} \quad (3.13)$$

There is no large difference between the two types of gearhead, but in the case of the planetary gearhead there is no 1:32 gearhead available, only 1:26 and 1:43. Also, these gearheads are twice the length of the spur gearheads and are twice as expensive. For these reasons, the spur gearhead is selected. The data sheet of the gearhead can be found in Appendix B. For the ball screw mechanism, a screw with a diameter of 12mm and a lead of 5 mm is selected and a tolerance

grade T9. The selected nut is a miniature single nut. the data sheet for both can be found in Appendix C

**Combination of motor and transmission** It has to be checked whether the requirements of the motor are met. The first one, highest calculated torque must be smaller than peak motor torque, is certainly met since that was the criterium for selecting the transmission ratio. For the second one the RMS value of the motor torque has to be calculated. First it has to be determined how the motor will be operated. Later in the chapter about the control will be explained that this will be with a constant speed. Because of this, the torque will rise linearly from the moment the motor starts to work until the unlocking phase. After this, the torque will drop back to 0 Nm at TO. During the swing phase the motor will not deliver a significant torque. We can put this in a graph and calculate the RMS value.

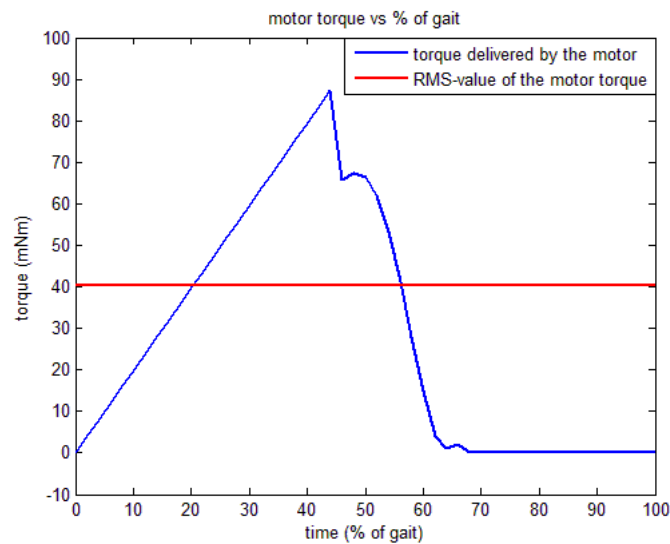


Figure 3.17: Torque delivered by the motor in blue and RMS value of the motor torque in red.

The RMS value of 40 mNm is inside the area of continuous operation of the selected motor so it meets both requirements. A problem with the motor however is that it should also be able to return to its original position in time during the swing phase. As this phase is about 30% of the gait cycle which is about 0.375 seconds and the spring is elongated over about 17 mm in total, the necessary rotational speed can be calculated:

$$\frac{17mm}{0.375s \times P} \times 60^{s/min} = 544^{rot/m} \quad (3.14)$$

This is normally no problem for the motor of 30 Watts since there is virtually no torque, only the rotational speed of the motor in continuous operation is limited by the chosen transmission ratio.

$$maximum\ speed = \frac{10000^{rot/min}}{32} = 312.5^{rot/min} \quad (3.15)$$

This means the motor has to be used at higher rotational speeds, which will cause the components to heat up more than normally. This shouldn't be a severe problem though, because the motor doesn't have to deliver a torque at this point. It will cause the lifespan of the motor to drop because of a higher loading of the bearings inside the motor.

The connection of the motor to the ball screw mechanism can be done through a belt or by directly attaching the motor shaft to the ball screw shaft. Using a belt causes additional losses but has the advantage that the motor and gearbox don't have to be placed in line with the ball screw mechanism. In this prosthesis however there is little space in between the foot bottom and the ankle axis since room is reserved for the locking mechanism. Because of this reason it is decided to place the motor and gearbox in line with the ball screw mechanism on the foot bottom.

### 3.4.3 Springs

The springs in this prosthesis design must have a high spring constant, they must provide a large force over a small extension. There are different types of spring that can be used: extension springs, compression springs, torsion springs, Belleville springs and a lot of other types. Extension and compression springs are the most common types, but the problem with these is that they get heavy and large with higher spring constants, and the same occurs with torsion springs. Belleville springs can provide a lightweight alternative for this, as it is possible to create a spring

with a high spring constant using a small amount of material in comparison to the other types. It is a small conical disc that has a high spring constant but only allows a small extension. By stacking these springs, the spring constant can be modified to customer needs.



Figure 3.18: Extension spring (left), compression spring (left middle), torsion spring (right middle), Belleville springs (right).

The spring constants can be calculated as explained before, using the MATLAB simulation. The choice of a spring constant is not predetermined if the pretension can be altered. Two springs with different spring constants can have a similar effect on the ankle. In Fig. 3.1 two springs with different pretensions are compared. By using this the spring constant and the pretension can be used to fit the sound ankle data.

Different spring constants are selected and the pretension is altered in order to get a good fit. This are the values that have been chosen:

spring	1	2	3
spring constant (N/mm)	20	200	200
pretension (mm)	10	4	12

Table 3.1: Initial choice of spring constants for the three springs.

A next step is to check what types of spring are suitable to provide such a spring. For all of the springs initially the comparison was made between extension springs, compression springs and Belleville springs. Especially for the larger spring constants, the Belleville springs seemed to be the best solution, but the big disadvantage of this type of springs is that they experience a lot of friction when stacked, which causes hysteresis with the loading and unloading, and this brings energy losses which cannot be neglected. If normal compression springs are compared to extension springs, it can be seen that extension springs take more space than compression

springs. For example, if the two types are compared for a spring of 200 N/mm and an extension of 10 mm, it is clear that the extension spring is larger than the compression spring. Dm is the diameter of the center line of the spring wire, Fn the maximum force, L0 the neutral length and Ln the length at maximum extension/compression.

	Dm	Fn	L0	Ln
extension spring	40	2000	44.2	34.2
compression spring	40	2000	82.3	92.3

Table 3.2: Comparison of extension and compression springs. Springs calculated at the spring calculation section of Alcomex' website: [www.alcomex.nl](http://www.alcomex.nl).

A specific type of compression springs seems very suitable for this application. The so called die springs are specially designed for dynamic loads and are more compact than normal compression springs. Another type with similar characteristics can be found in rubber or elastomere springs. This type however has higher spring constants for the same dimensions, which cause the die springs to be a more compact solution.

An easy solution would be to use torsion springs on the ankle joint. Most stores that sell torsion springs only offer them with wire thicknesses up to 3 mm, with maximum torsion stiffnesses of about 100 mNm/°, which is a factor 10 too small even for the first spring. The characteristics of torsion springs can be calculated for different wire thicknesses to check if the springs needed for this application would have acceptable dimensions to fit on the ankle joint. For a given material, wire thickness, spring constant and loading force the stress due to bending can be calculated in the torsion spring.

$$\sigma = \frac{M}{\left(\frac{\pi}{32} \times d^3\right)} \quad (3.16)$$

Where M is the torque applied and d is the wire thickness. The number of windings can also be calculated from these variables:

$$n = \frac{d^4 \times E \times \alpha \times \pi}{360 \times 32 \times Dm \times M} \quad (3.17)$$

Where E is the spring's material's Young modulus,  $\alpha$  is the angle over which the spring is rotated and Dm is the diameter of the center line of the spring wire. These values can now be



calculated for the first spring, knowing that the spring constant needed is 1 Nm/°, Dm is chosen 20 mm, the maximum angle is 5° if the spring is only active in one direction, the Young modulus of the material is 206 Gpa and the maximum bending stress for the wires is equal to:

$$\sigma_{max} = 0.7 \times (2220 - 820 \times \log(d)) \quad (3.18)$$

d (mm)	2	3	4	5
$\sigma$ (Mpa)	6366	1886	795	407
$\sigma_{max}$ (Mpa)	1381	1000	1208	1153
n	0.04	0.23	0.72	1.7

Table 3.3: Stress, maximum stress and number of windings for a spring with  $c=1$  Nm/° and different wire diameters.

The spring can be replaced by a very compact torsion spring with a total length of less than 2 cm if a wire diameter of 5 mm is taken. This spring can also be split into two springs with  $c=0.5$  Nm/°, so they can be attached at both sides of the prosthesis to get a symmetrical load. The same can be checked for spring 2, which needs a spring constant of 9 Nm/°, and the calculations show that the torsion spring would need a wire diameter of 11 mm and more than 5 windings, which makes the spring too large and heavy to fit on the ankle joint.

#### 3.4.4 Locking mechanism

Two locking mechanisms are needed, one to lock the orientation of the small lever arm to that of the leg and one to lock the orientation of the large lever arm to that of the foot. For the locking mechanisms a pawl-ratchet mechanism can be used. This has two positions: when open, a rotation in both directions is allowed, and when closed a rotation in only one direction is allowed. There are two problems with using this mechanism, and one of them is the resolution. The mechanism will be only able to lock on a limited number of lever arm angles. If the position of the lever arm is a fraction further than one of these angles, the lever arm locks at the next possible position and a lot of energy will be lost. Moving the locking mechanism further away from the ankle axis is not a good solution, although this makes that there is more room for the same angle, it also raises the forces on the mechanism so that the mechanism will have to be heavier and take more space. That is the other problem, at least for the large lever arm, which

has to be unlocked when the forces on the locking mechanism are high. This would require a servo motor that can overcome the high friction forces in order to unlock.

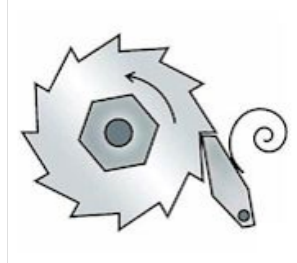


Figure 3.19: Pawl-ratchet mechanism in locked position. The ratchet can only rotate in the direction of the arrow.

A first solution for the resolution problem is to provide several pawl-ratchet mechanisms for each lever arm, each of them shifted a bit. For example if three parallel mechanisms are used, the resolution can be up to three times as high. The placement of these mechanisms takes a lot of room in the prosthesis since all of them have to be designed to withstand the forces too. This is also not a good solution for the high friction at unlocking.

Another solution is to use a transmission between the lever arms and the locking mechanisms. The advantages here are that the resolution will be higher and the forces on the locking mechanism will be lower, so this solves both of the problems that occurred. A disadvantage of this is that the friction losses in the locking mechanism will be amplified on the lever arm.

A third possible solution is to use a mechanism with a singularity at the locking position. An example of a mechanism of this kind is recently developed at the university of Twente. The advantage of this mechanism is that it only needs a small force to unlock and there is not much friction when the mechanism is unlocked. The disadvantage is that there is only one angle, being the position of the singularity, where the mechanism locks. This makes it suitable for a knee joint where  $0^\circ$  is where the locking happens, but for the small lever arm in the prosthesis the locking position can vary when it is used on leveled terrain for example. The large lever arm locking position however is not influenced by changes in slope of the terrain or anything else, and this type of locking mechanism could be used for it. The problem that remains however is that when the lever arm doesn't completely return to its initial position, there is no locking and so there is no additional energy for push-off [11].

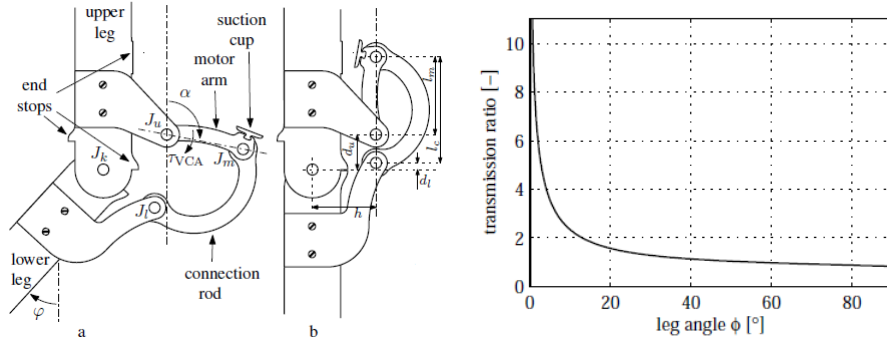


Figure 3.20: Example of a singular state locking mechanism in unlocked (a) and locked position (b), and an example of the transmission ratio versus the angle (right). The mechanism is applied to a knee joint in this case.

Based on the comparison between the different mechanisms, the pawl-ratchet with a transmission is preferred over the other ones. The research on the locking mechanisms and the design of the transmissions is currently still ongoing (Cherelle et al. (in progress)). The locking beyond the scope of this thesis.

### 3.4.5 Conclusions

The components that are selected are:

- A Maxon EC 45 flat motor with a rated power of 30 W
- A Maxon Spur Gearhead GS 45 A with 3 stages and a transmission ratio of 32:1
- A Bosch ball screw mechanism with a screw diameter of 12 mm and a lead of 5mm, together with a Miniature Single Nut with Flange FEM-E-B
- Two die springs with a spring constant of 200 N/mm, an inner diameter of 16 mm and an outer diameter of 32 mm.
- Two torsion spring with a spring constant of 0.5 Nm/° and a wire thickness of 4mm.

## 3.5 Control and electronics

### 3.5.1 Sensors

Two different categories of sensors can be distinct: the sensors that are necessary for the operation of the prosthesis and those that perform measurements to check to what extent the prosthesis performs as has been predicted by the simulations.

### 3.5.2 Sensors for operation

In order to make the prosthesis work as it is supposed to do, the motor and the lockings have to be activated and deactivated at the right time. For this, sensors are needed to evaluate in which part of the gait cycle the prosthesis is at any given time and an algorithm is needed to organise what should happen at what time. There are 3 components that have to be controlled, being the motor and the two locking mechanisms. To define how many and which sensors are necessary, the prosthesis operation is subdivided in different phases, starting a new phase every time the state of one of the 3 components has to change. In Table 3.4, these phases are compared with the gait cycle events.

gait cycle event	phase	motor state	locking small lever state	locking large lever state
IC	1	on	unlocked/locked	locked
FF	1	on	locked	locked
HO	2	on	locked	unlocked
TO	3	reversed	unlocked	unlocked

Table 3.4: Subdivision of the prosthesis operation in different states.

Based on Table 3.4, three events have to be observed in order to be able to control the prosthesis. A first one is when the heel touches the ground for the first time, so the motor can be started and the storing of energy in the spring can begin. At this point, the large lever arm has to be locked in order to be able to store energy. The state of the small lever is not important since the leg rotates in the direction which is never obstructed by the locking mechanism. Ideally this locking mechanism should be unlocked here to reduce the losses due to friction, but since these losses should be small and having the mechanism locked here means less sensors are needed, it is a good idea to keep it locked. A second event is when the heel leaves the ground. Obviously, this can be measured by the same sensor as in the first phase. In this phase the large lever arm

is unlocked and the stored energy is released. A last sensor has to notice when the toe leaves the ground, so that the motor can be put in reverse and the small lever can be unlocked so the prosthesis can return to it's initial position.

There are several types of sensors that could be used to sense the ground contact. A first type are force sensing resistors. These sensors give a signal when a force is applied on it's surface. The problem with these is that their readings turned out to be unreliable on earlier prototypes, and that they are not proof against the high forces that are applied to them when they are attached to the foot sole [5]. Another possible sensor makes use of a contact switch to determine whether there is contact or not. This is a simple type of sensor with a simple high or low output, which makes it easier to interpret the readings. The problem with this type is that it is also not resistible to high forces, so not suitable to attach to the foot sole or to let the contact switch stick out below the foot sole. This can be solved by attaching a lever to the sensor which then pushes the contact switch. Because the sensor lever should not stick out of the foot contour since it might get damaged, a hinging sensor plate is attached to the heel. For the sensor that measures the toe contact this is not necessary, because the toe joint can be used to push the sensor switch. The sensor has to be placed in such a way that it gives a high value when the toe joint is lifted up and a low one when it's down. The motor control than has to use the transition from high to low to reverse the motor. These sensors are very cheap and compact. An example of a sensor that can be used in the prosthesis is the Cherry Ultramin microswitch, shown in Fig. 3.21.



Figure 3.21: Cherry Ultramin microswitch.

The control algorithm for the prosthesis is presented schematically in Table 3.5. It is a very

simple algorithm using only two sensors to control both of the lockings and the motor.

time (gait cycle event)	IC	MDF	TO
sensor reading	heel sensor high	heel sensor low	toe sensor high -> low
commands given	motor rotates forward, small lever arm locked, large lever arm locked	large lever arm unlocked, motor changes speed	motor reversed, small lever arm unlocked

Table 3.5: Control algorithm for the prosthesis.

**Sensors for measurements** The prosthesis' performance has to be compared to its simulation and to the sound ankle gait data. To be able to do this the ankle angles and torques must be measured. Other things that can be measured to verify the performance are the lever arm locking positions, to check if the lockings work as they are supposed to work. Measuring these things make it easier to detect prosthesis malfunctioning and localise the problem. Because adaptations still have to be made on the ankle joint in order to fit the locking mechanism on it, and so the available space is unknown, these sensors couldn't be permanently chosen.

**Angle measurement** For the measurement of the angles a rotary encoder can be used. There are two main types we can distinguish: absolute and relative encoders. The difference between the two types is that in absolute encoders both the actual angle, changes in angle and the direction of change can be observed, whereas relative encoders only observe changes in angles. For the measurement of the ankle angles, it is not really necessary to have an absolute encoder.

**Torque measurement** The measurement of the ankle torque can be accomplished in several ways. A first method is measuring the ground reaction forces. This is how the data of the sound ankles were recorded. The problem of this method is that it requires an accurate model of the prosthesis in which the measured forces have to be used as input to determine the torques. If the model is not completely the same as the actual prosthesis, the torques will not be the same as the actual torques. Another method is to measure the extension of one of the springs, calculate the force and from that the torques. One way to do this is to measure the difference in

angle between the lever arms and the leg, which can also be done by a rotary encoder.

### 3.5.3 Motor control

The motor has got three Hall sensors which are placed at  $120^\circ$  of each other and indicate the rotor position. These three sensors divide the revolution in six different phases, based on their readings. The motor has 3 windings which are arranged in such a way that six different conducting phases are created which overlap with the sensor phases. An overview of this principle can be found in Fig. 3.22. The applied voltages are block-shaped, and so are the currents.

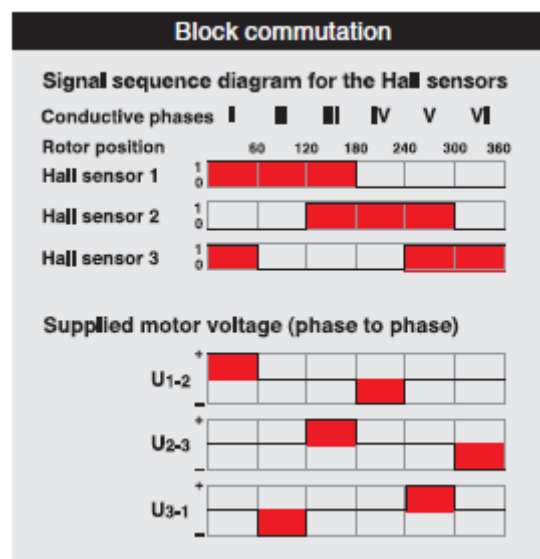


Figure 3.22: Hall sensor signals and supplied motor voltage for a Brushless DC motor. Image adapted from Maxons “Technology- short and to the point” data sheet.

In order to apply the right voltage at the right time, an electronic circuit is necessary which uses the sensor readings to regulate the voltage. This can be done in several ways, but there are electronic components available which control this block commutation. If these are used, it is very easy to regulate the rotational speed and sense of rotation of the motor. An electronic circuit for the control of the Maxon EC 45 flat has been created in a previous thesis work for the driving mechanism of a soccer playing robot, using an L6235 chip. This circuit could be used in this case too [22].





$$V_{stance1} = \frac{\omega}{c} = \frac{8000rpm}{374rpm/V} = 21.4V \quad (3.20)$$

Between the unlocking of the lever arm and and TO, the spring is extended over another 4 mm in order to reach a torque of 0 Nm at an angle of -20°.

$$\omega_{stance2} = \frac{3mm}{5mm \times 0.245s} \times 32 \times 60s/h = 4700rpm \quad (3.21)$$

$$V_{stance2} = \frac{\omega}{c} = \frac{6270rpm}{374rpm/V} = 12.6V \quad (3.22)$$

For the swing phase, the same calculation can be performed.

$$\omega_{swing} = \frac{16mm}{5mm \times 0.375s} \times 32 \times 60s/h = 16400rpm \quad (3.23)$$

$$V_{swing} = \frac{\omega}{c} = \frac{16400rpm}{374rpm/V} = 43.8V \quad (3.24)$$

Knowing that the motor needs time to reverse its sense of rotation too, these values will have to be slightly higher than calculated here. The mechanical time constant however is very small (17 ms), so this will not have a large impact.

This voltage seems very high, but the motor is able to withstand a voltage larger than the maximal voltage for continuous operation. The consequence of this is that the lifespan of the motor will drop. Also for the L6235 chip it's not a problem since it works up to 52V. Some measures can be taken to lower this rotational speed and voltage.  $\omega_{stance2}$  can be reduced, with the effect that after powered PF, when the torque is back to 0 Nm, the angle will not be -20° but rather to -16° or -17°. This seems to have only a very small effect on the gait cycle, as can be seen in Fig. 3.24. For this result,  $\omega_{stance2}$  was reduced to 1500 rpm, which means an extension of 1 mm rather than 3 mm. The result of this is that  $\omega_{swing}$  is reduced to 14000 rpm and  $V_{swing}$  to 37V. In Fig. 3.24 the torque becomes negative for angles smaller than -16, but in reality this will not happen. This is caused by the fact that the angles are used as an input in the simulation.

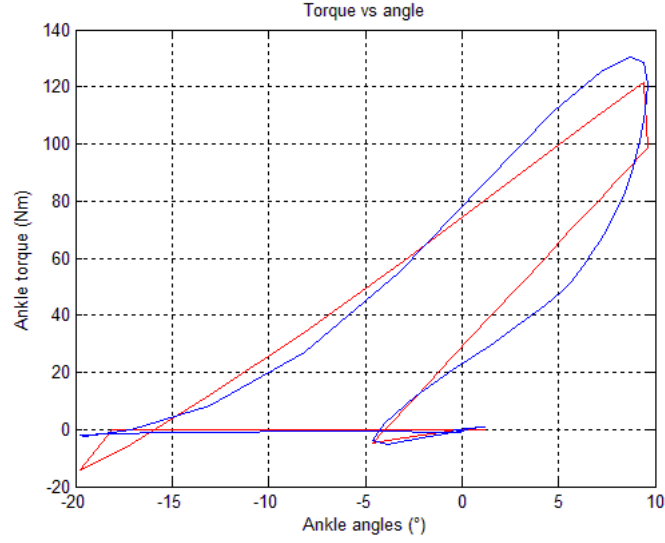


Figure 3.24: Result of the simulation of the prosthesis with a reduced rotating speed during powered PF.

#### 3.5.4 Motor autonomy

The required amount of batteries can be calculated from the motor operation and its characteristics. The torque characteristic of the motor throughout the gait is known, so from this the current can be calculated using the torque constant that is given in the motor data sheet.

$$I = \frac{T_{motor}}{c} = \frac{T_{gearbox} \times R}{c \times \eta_{gearbox}} = \frac{(F \times \frac{P}{2 \times \pi \times \eta_{ball screw}} \times R)}{c \times \eta_{gearbox}} \quad (3.25)$$

Where  $I$  is the motor current,  $T_{motor}$  is the torque at the motor outlet shaft,  $c$  is the torque constant of the motor,  $T_{gearbox}$  is the torque at the gearbox output shaft,  $R$  is the transmission ratio of the gearbox,  $F$  is the force acting on the spring that is loaded by the motor,  $P$  is the ball screw lead and  $\eta$  is the efficiency.

It is hard to know the value of the torque during the swing phase because the forces on the spring,  $F$  in Eq. 3.25, is around 0 here. An estimate is made of 0.001 Nm for the torque. This torque will clearly be low in comparison to the torque during stance since there is no elongation of springs. The motor current throughout the gait cycle is shown in Fig. 3.25.

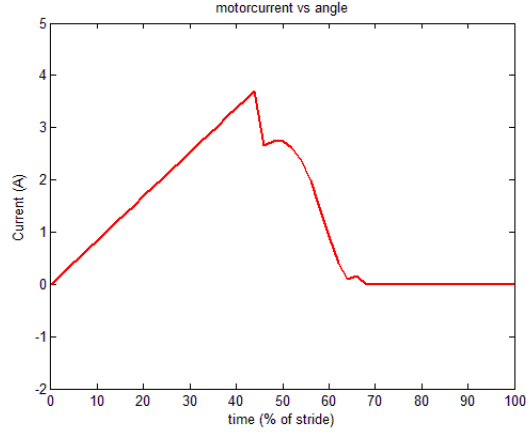


Figure 3.25: Motor current vs the % of the gait, calculated with Eq. 3.25.

If this current is multiplied by the motor voltage, the electrical power consumption of the prosthesis is calculated. By multiplying this curve with the voltage in each phase, being 21,4V between IC and MDF, 16.8 between MDF and TO and 49.5V during swing, and then computing the integer of graph, the energy consumption per step is calculated. The energy necessary to start up the motor has to be added to this value twice, since the motor starts up twice every step, once on IC and once on TO. This can be calculated from the current on startup and the mechanical time constant that can be found in the data sheet.

$$E_{startup} = V_{nom} \times I_{start} \times t_{start} \quad (3.26)$$

With  $E_{startup}$  the energy consumption during motor startup,  $V_{nom}$  the nominal voltage of the motor,  $I_{start}$  the starting current of the motor as found in the data sheet and  $t_{start}$  the mechanical timeconstant as found in the data sheet.

$$E_{step} = E_{stance} + E_{swing} = \int V_{stance} \times I_{stance} dt + \int V_{swing} \times I_{swing} dt + 2 \times E_{startup} \quad (3.27)$$

With  $E$  standing for the energy consumption,  $V_{stance}$  and  $I_{stance}$  the motor voltage and current during stance,  $V_{swing}$  and  $I_{swing}$  the motor voltage and current during swing.

$E_{stance}$	$E_{swing}$	$E_{startup}$	$E_{step}$
24.2 J/step	0.3 J/step	2 J/startup	28.5 J/step

Table 3.6: Energy consumption during one step in the different phases.

The value of 24,2 J/step could have been predicted from the efficiency of the driving system and the energy input in a sound gait cycle as calculated in Eq. 1.5. Since the motor has to provide the same amount of energy and the total efficiency of the driving system is about 70%, we get this equation:

$$E_{stance} = \frac{E_{healthy\ ankle}}{\eta_{driving\ system}} = \frac{16.6}{0.7} = 23.7 \quad (3.28)$$

Which gives about the same value for both calculation methods.

In order to calculate the necessary battery mass, two things have to be known. The first is the number of steps a person should be able to take with his prosthesis without running out of energy. The second is the number of energy a battery can deliver for a certain battery mass.

The type of batteries with the highest energy density are Lithium-polimere batteries, with an energy density of up to 200Wh/kg. The number of steps one takes each day is very dependent on the kind of person, the age, the job, ... A range from 5000 to 20000 steps a day seems realistic though. This would lead to a range of 145.5 to 582 kJ or 40 to 160 Wh. So, depending on the amputee, 200g to 800g of batteries would be necessary. It would be possible to provide different sized packs of batteries for different tasks, so that amputees could fulfill basic tasks with a light battery pack but also have the possibility to have a longer motor autonomy with a larger battery pack.

### 3.6 Prosthesis design

The design of the prosthesis parts is done in Autodesk Inventor Professional 2011. First, a design was made using the maximum possible dimensions of the prosthesis, to get an idea of what was possible in the arrangement of the different parts and components. A first stress analysis was

performed on the parts to roughly know the necessary dimension to withstand the forces. Then the arrangement that would be as compact as possible was chosen and the parts were designed to use less material and fit in the prosthesis. Different variables in the prosthesis simulation, like the spring stiffnesses and pretensions, lengths of the lever arms and spring connection points, were varied in order to optimise the design without affecting the prosthesis' characteristics.

### **3.6.1 Initial design phase**

In the first phase of the design, some different arrangements were tried out. The design started by creating a foot structure with dimensions as large as acceptable: a height of 90 mm to the ankle joint, a width of 100 mm and a length of about 250 mm. This is an estimation, based on the dimensions of a sound foot. Several difficulties that had to be solved became clear during this phase:

- The motor and gearbox, in line with the ball screw mechanism would have to fit on the foot sole together with the two die springs, which have an outer diameter of 32 mm and a length of about 38 mm. Since the motor has a diameter of 45 mm, placing the springs next to the motor would almost cause the whole 100 mm of available space in the width of the prosthesis to be taken. This would clearly not lead to a compact design.
- The springs have to be attached to the lever arms or the ball screw nut. Since the springs should be loaded symmetrically and not under an angle, this requires a lot of pulley mechanisms or, ideally, the springs to be placed in such a way that few pulleys as needed, so in line with the lever arm or ball screw.
- The lever arms that are connected to each other should also be loaded as symmetrically as possible to avoid out of plane deformation.
- The deformation of the foot bottom plate has to be as small as possible, since the tolerance on radial displacement for the ball screw mechanism is very small.
- Allowing an inversion and eversion movement in the prosthesis, which would bring the prosthesis behaviour closer to that of a healthy angle, is very hard with this concept. Normally this rotation happens in between the ankle joint and the foot bottom, and allowing

this would cause lever arms and motor axis to collide. There are other options to provide this movement. A first one is to allow a rotation in the frontal plane above the ankle joint by adding a second joint with a narrow range of rotation. A second one is to attach a rubber strip at the bottom of the prosthesis. Both of these could allow a small change in angle in the frontal plane.

- The locking mechanisms for both of the lever arms would be placed on the ankle axis. After considering the possible options, the prosthesis was made less wide at the ankle joint so that the locking mechanisms could be placed on both sides of the prosthesis, on the outside of the foot connected to the ankle axis.

### **3.6.2 Final design**

The different parts of the prosthesis will now be described as will the results of a stress analysis. For a better understanding of the design motivations, first the design and the arrangement of the parts will be described and the stress analysis will be done afterwards.

**Final arrangement** The motor and gearbox, in line with the ball screw assembly are placed in the center of the prosthesis on the foot bottom plate. The side of the prosthesis is made of two sagittal structures which support the ankle axis as can be seen in Fig. 3.26.

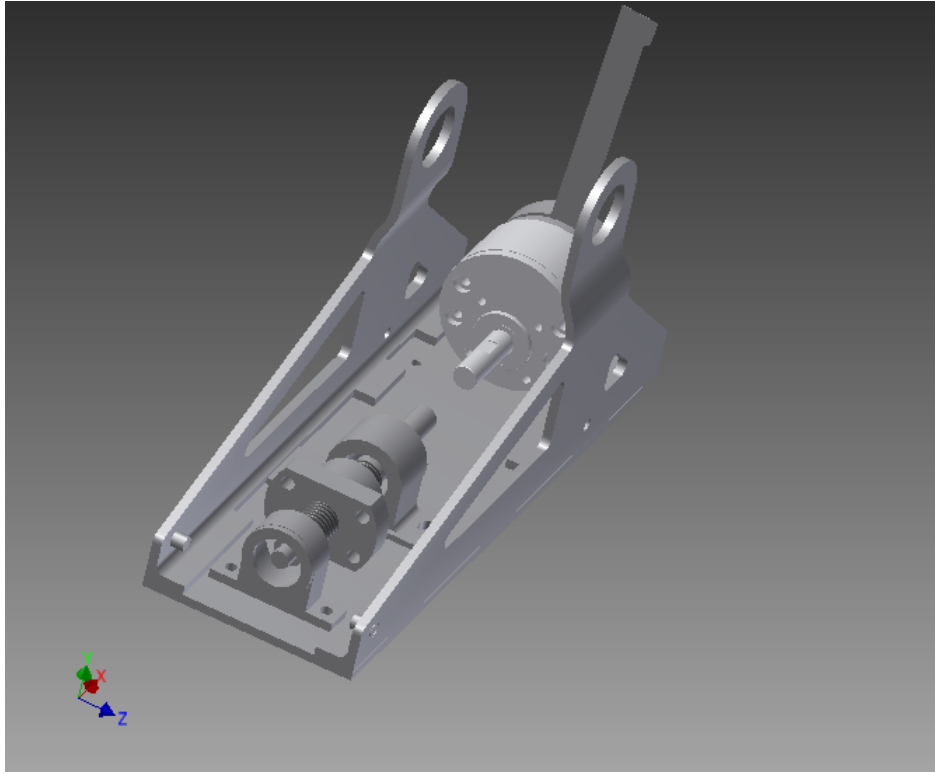


Figure 3.26: The foot sagittal and bottom structure, with the motor and gearbox at the back and the ball screw assembly with the screw, nut and two pillow blocks.

The gearbox is attached to the foot bottom by means of a structure which is connected both to the gearbox and the foot bottom with bolts. The motor axis is connected to the ball screw axis and the spring that is elongated by the motor is placed over this connection. Both sides of this spring are connected to cables, one side to be connected to the ball screw nut, the other side to be connected to the large lever arm. The spring is placed over an axis which has to prevent it from moving and hitting the motor or ball screw axis when compressed (Fig. 3.27). The axis is connected to the gearbox connecting structure on one side and to the ball screw bearing on the other side.

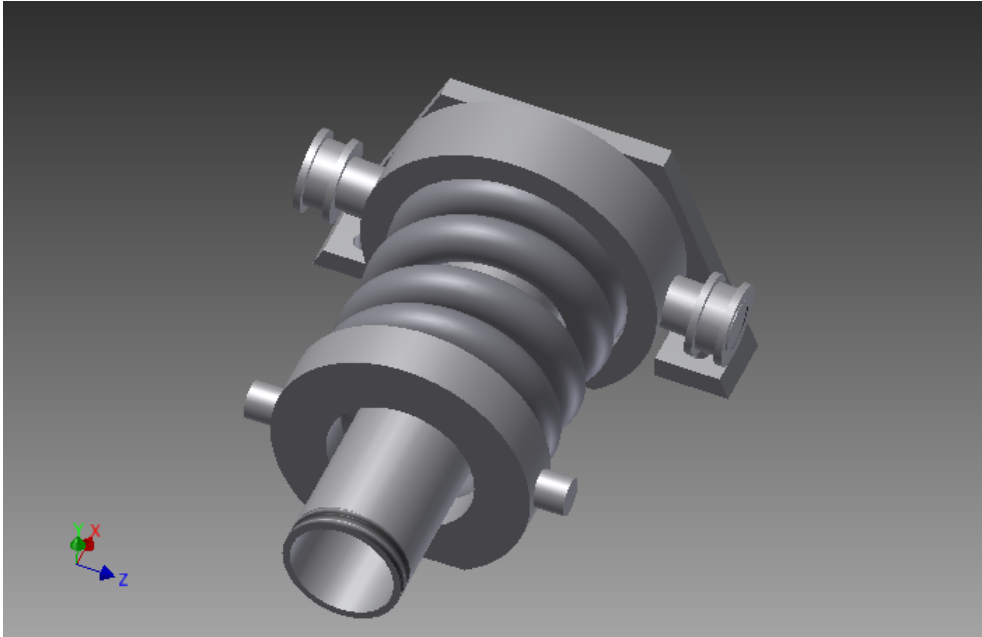


Figure 3.27: The spring that is placed over the motor-ball screw connection.

A structure is connected to the ball screw nut that allows to connect a wire from the nut to the spring. This wire can be directly connected to the spring, without the need for pulleys (Fig. 3.28).



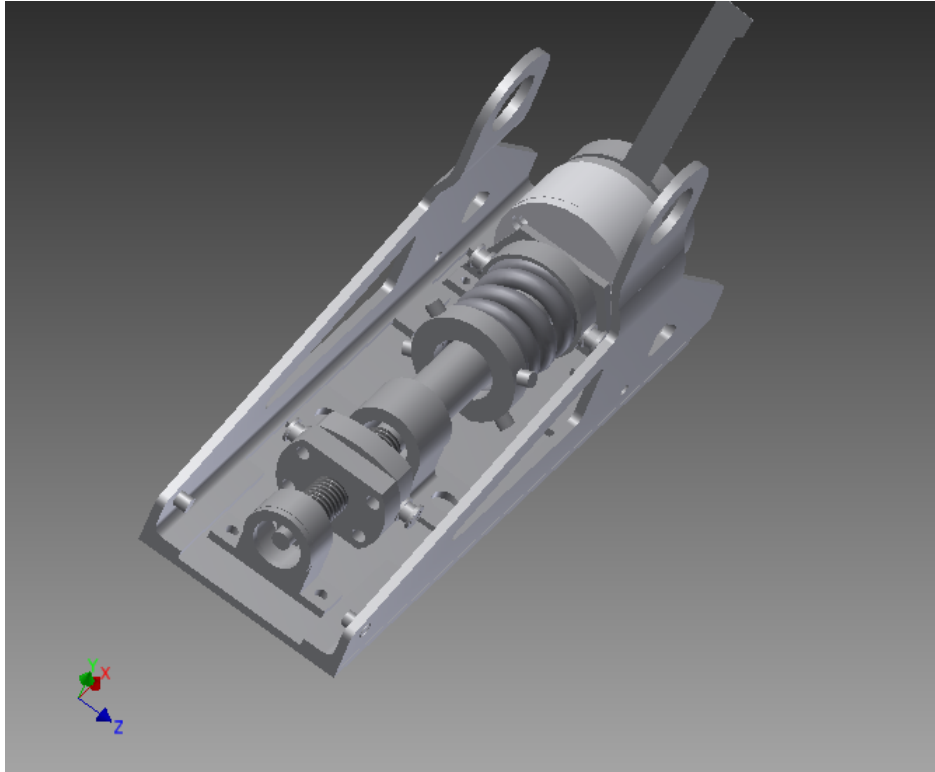


Figure 3.28: The prosthesis structure with the driving system and one of the springs.

On the ankle axis the two lever arms are connected. The large lever arm is placed in the center. The end of the lever arm is split in two parts to fit around the ball screw assembly, and to be able to load the spring symmetrically. The small lever is split into two parts, one on each side of the large lever, again to have a symmetrical load and to avoid out of plane deformation (Fig. 3.29).

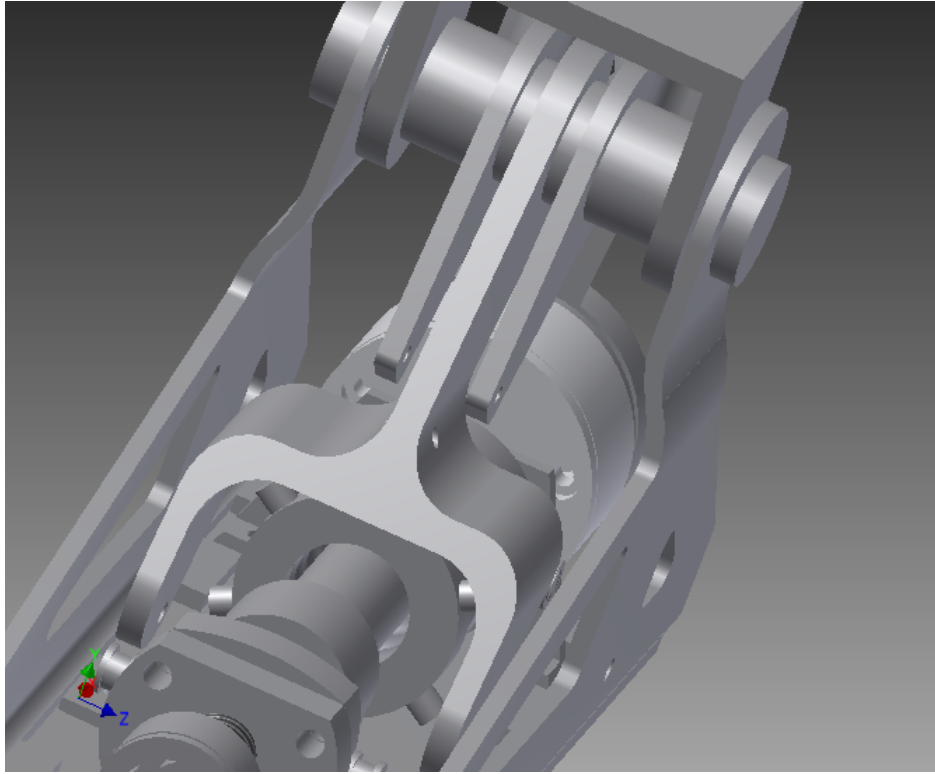


Figure 3.29: The two lever arms, connected to the ankle axis and placed over the driving system axis.

The large lever cannot be directly connected to the spring, because the forces would be acting in the wrong direction. Pulleys are placed on each side of the center to connect the lever to the spring in a correct way (Fig. 3.30).

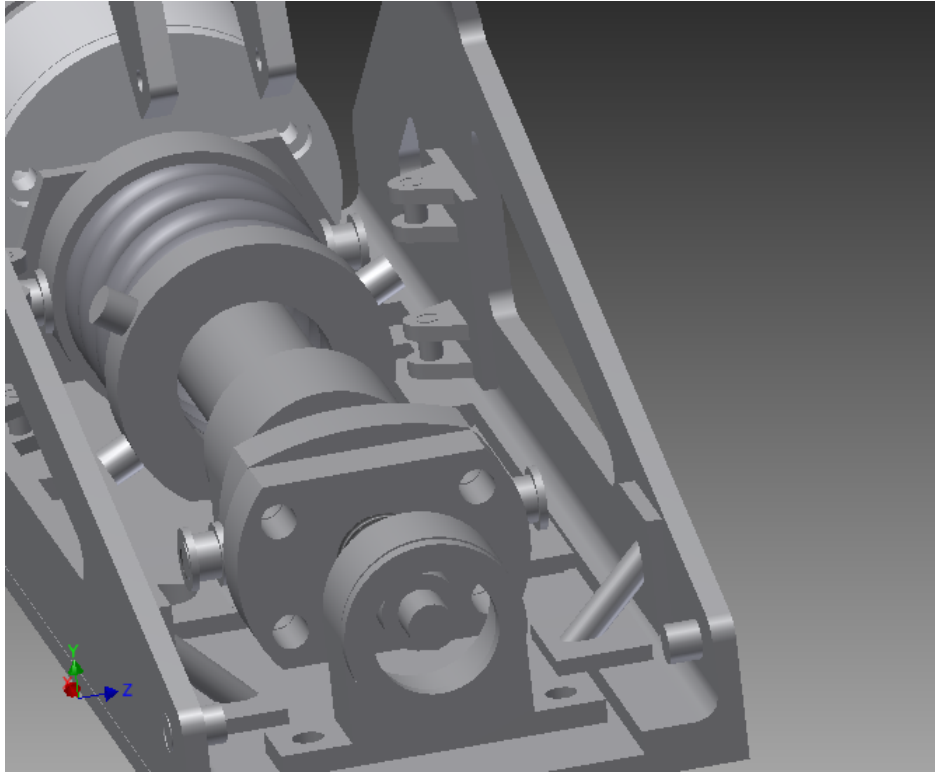


Figure 3.30: The pulleys attached to the side structure of the prosthesis.

The spring for the controlled DF is placed on the small lever arm, on the back side of the prosthesis. The end of the spring is connected with the steel wires that go over the ankle axis and connect the small lever to the large lever. The torsion springs are placed on the ankle axis and connected to the leg and the large lever arm (Fig. 3.31).

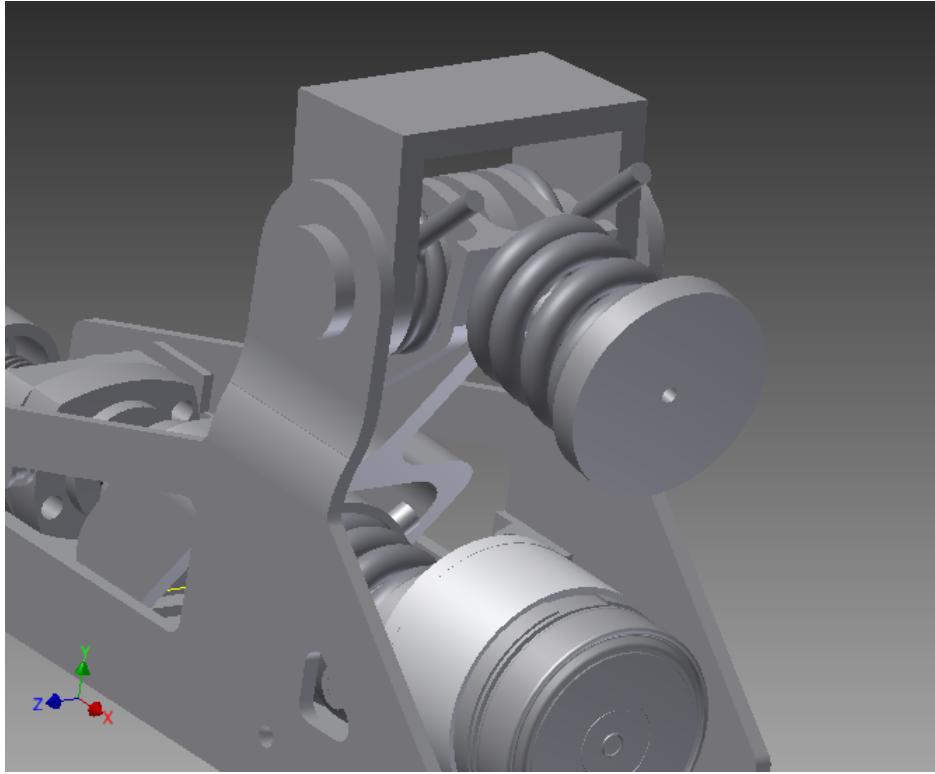


Figure 3.31: One of the springs, attached to the small lever arm and placed at the back of the prosthesis, and two torsion springs placed on the ankle axis.

Finally, a toe joint is connected to the front of the prosthesis and the heel sensor plate is connected to the back (Fig. 3.32).

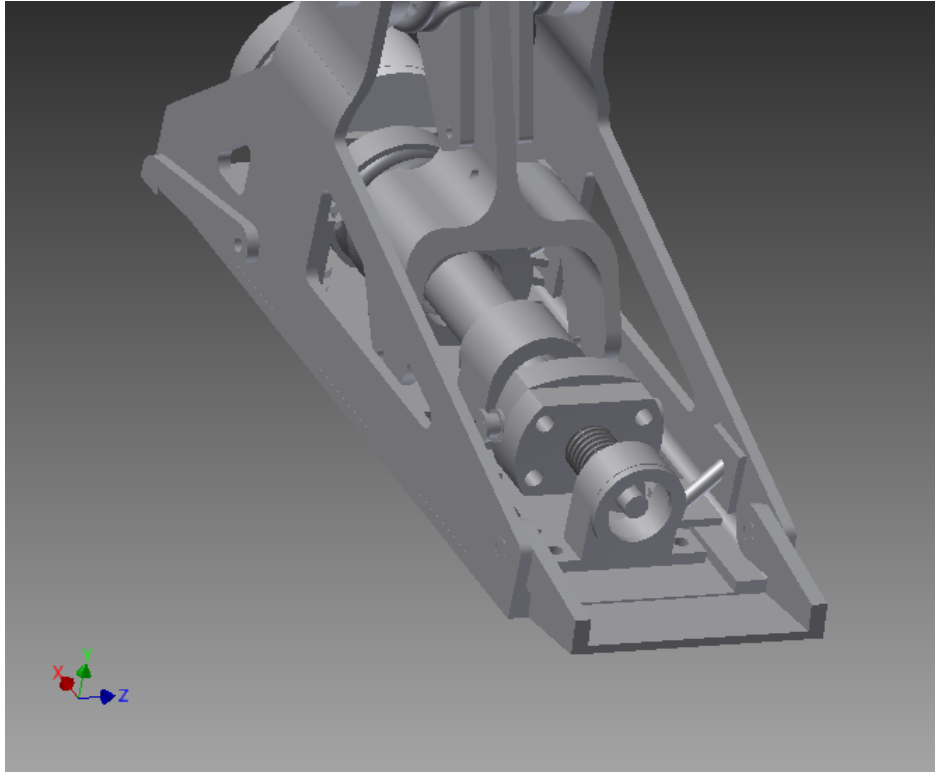


Figure 3.32: Toe joint and heel sensor plate are placed at the front and the back of the prosthesis.

The locking mechanisms are not added to this model since they are still in a research phase. Also, the ankle axis will need further adjustments when the design of the locking mechanisms is completed, so the connection of the torsion springs cannot be definitely decided. The small recall spring returning the large lever arm to it's initial position is not drawn either.

**Different phases** To get a better view on the operation of the design, a short overview of the different phases will be illustrated by means of figures of the design. The prosthesis' arrangement will be shown for the main gait events in Fig. 3.33 to Fig. 3.36. The figures are made from the same angles so that the changes in arrangement are easier to notice.

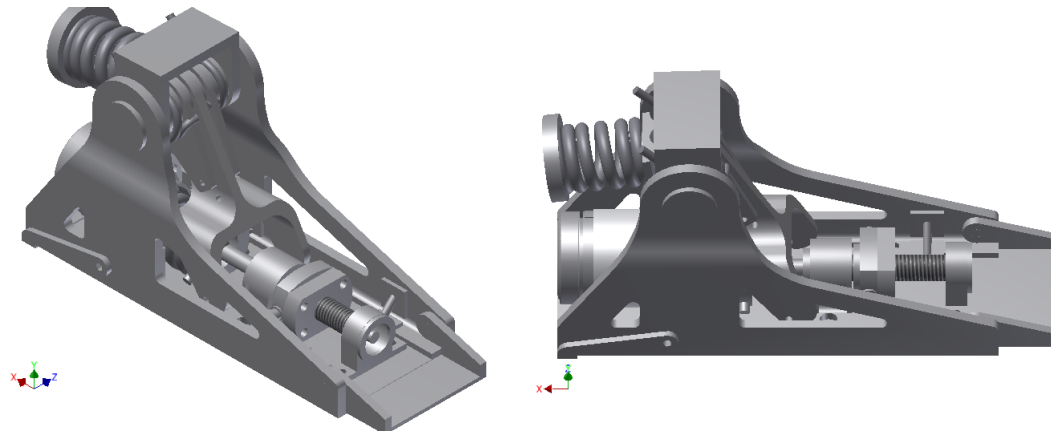


Figure 3.33: The prosthesis' arrangement at IC. The lever arms and the ball screw nut are in their beginning position, the leg has an angle of  $0^\circ$ .

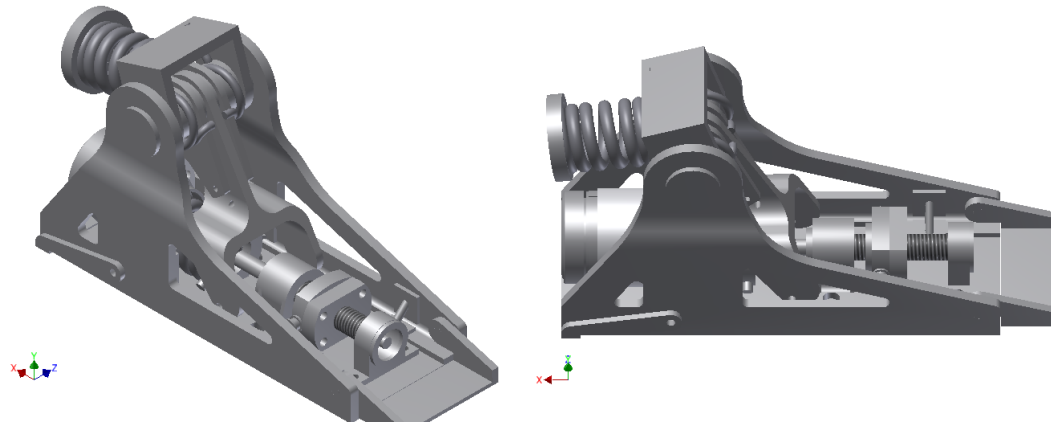


Figure 3.34: The prosthesis' arrangement at FF. The leg is at  $-5^\circ$ , loading the torsion springs. The small lever arm is in its beginning position, the ball screw nut is compressing the spring positioned over the motor axis.

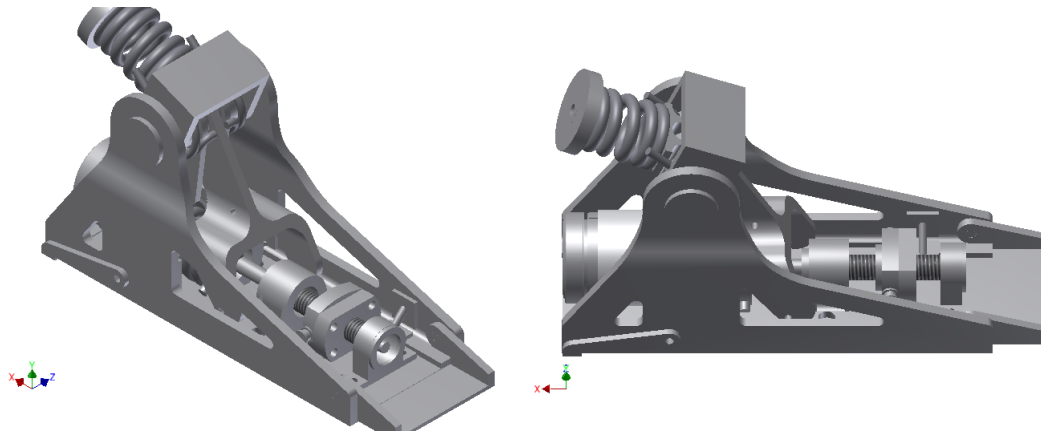


Figure 3.35: The prosthesis' arrangement at MDF. The leg is at  $10^\circ$  and the small lever arm rotated over  $15^\circ$ , compressing the spring positioned at the back of the prosthesis. The ball screw nut is still compressing the spring positioned over the motor axis.

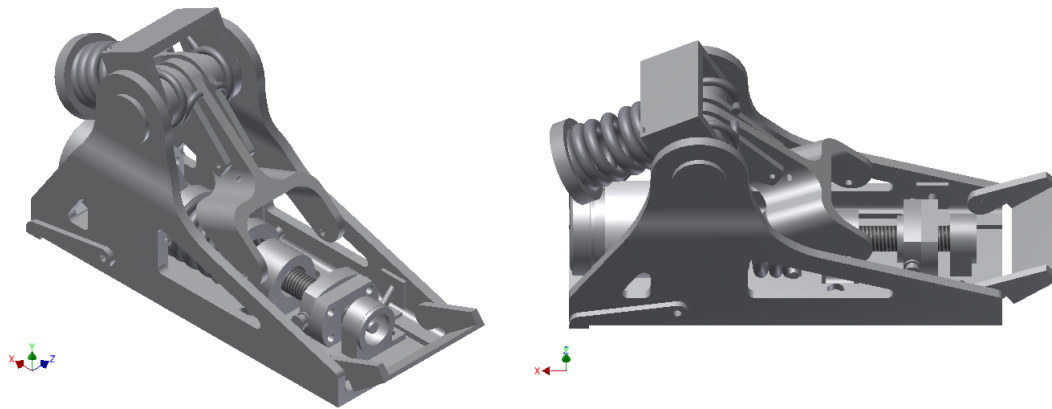


Figure 3.36: The prosthesis' arrangement at TO. The locking mechanism blocking the large lever arm is unlocked, the large lever arm rotated over an angle of about  $-20^\circ$ . The small lever arm rotated over an angle of  $30^\circ$  and the ball screw nut is at its ultimate position. The toe joint is lifted because only the toe of the prosthesis has ground contact. The small torsion spring that has to be used to return the toe joint to its original position is not drawn. A small recall spring attached to the large lever arm returns the arrangement to the initial position after this.

**Part design** The final design of the different parts will now be explained. The forces acting on the parts are calculated and a stress analysis is performed. The material used for the calculations is the default Aluminium type in inventor, being Al 6061. The properties of this material are written down in Table 3.7.

property	mass density	yield strength	ultimate tensile strength
value	2.71 g/cm <sup>3</sup>	275 MPa	310 MPa

Table 3.7: Properties of Al 6061 (Autodesk Inventor database).

For all of the parts, the stress calculations are done with the highest loads that occur. The safety factor is defined as the maximum stress divided by the yield strength. The calculations are first done for a static load, afterwards an extra safety factor is applied if the loads are dynamic, which is the case for most of the parts. The extra safety factor depends on maximum stress limit for an infinite number of loading cycles when fatigue occurs. This maximum stress is different for different loading conditions. Table 3.8 gives the stress limit and the safety factor for the different loading conditions for Al 6061.

loading conditions	static (Yield strength)	Bending fatigue	Axial fatigue	Torsion fatigue
Maximum strength (MPa)	260	232.5	216	154
safety factor	1	0.89	0.83	0.59

Table 3.8: Additional safety factors for different dynamic loading conditions.

**Large lever arm** The large lever is connected to the ankle axis under an angle of 30° when locked. There are two loading conditions that are looked at, one just before unlocking, when the forces on the bottom connection point, connected to the motor loaded spring, are maximal, and just after unlocking, when the forces on the top connection point, connected to the small lever arm, are maximal. The maximum force due to the motor loaded spring is 2600 N. At this point, the forces between the small lever arm and the large lever arm are 2326 N. These values are calculated in the prosthesis simulation. Also, the angles of the forces can be calculated there, but for this case the forces can be approximated with forces in the transverse plane. It can be seen in the simulation that this is a good approximation, for example the 2600 N is really 2584 N in the transverse plane and 290 N perpendicular to this plane. This last force only has a small effect on the lever arm.



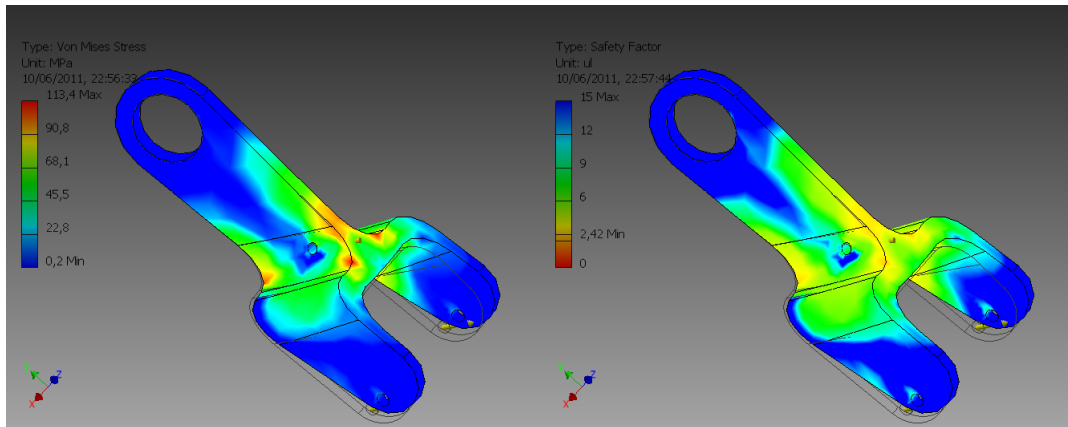


Figure 3.37: Visualisation of the stress (left) and the safety factor (right) in the first loading case of the large lever arm: before unlocking.

After the unlocking, the forces change to 1680 N on the bottom of the large lever and 2800 N between the large and the small lever.

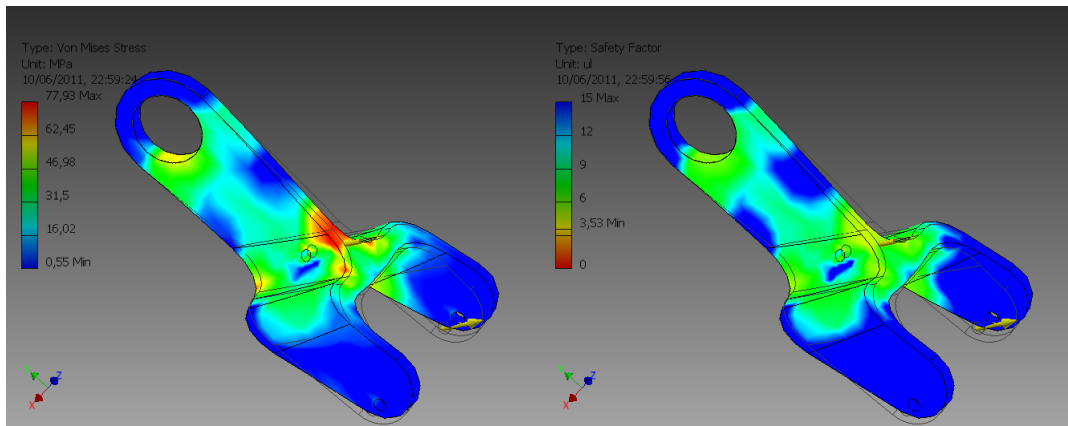


Figure 3.38: Visualisation of the stress (left) and the safety factor (right) in the second loading case of the large lever arm: after unlocking.

Since in this case the lever is submit to axial and bending conditions, the lowest safety factor of the two is taken. The static safety factors now have to be multiplied with this dynamic safety factor to get the total safety factor. Since the stresses before the unlocking were the highest, this is the most critical of the two. The total safety factor for this part is:

$$S_{total} = S_{static} \times S_{dynamic} = 2.81 \times 0.83 = 2.28 \quad (3.29)$$

**Small lever arm** The small lever arm is also connected to the ankle joint under an angle of  $30^\circ$  when locked. The maximum force working on the lever arm is the 2800 N after unlocking, the same as for the large lever. This load is both applied at one end of the lever arm where the spring is attached as on the other end where the steel wire is connected to the large lever arm. On the spring end, the load is simulated as a pressure rather than a force. The force is divided by the area where the spring has contact with the lever arm.

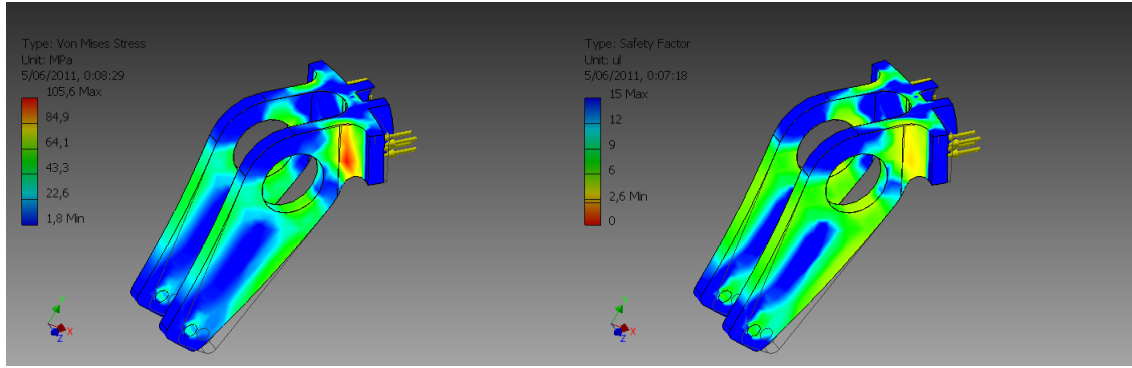


Figure 3.39: Visualisation of the stress (left) and the safety factor (right) in the highest loading case of the small lever arm: after unlocking.

The loading conditions are bending and axial like in the previous case, so the total safety factor becomes:

$$S = 2.5 \times 0.83 = 2.08 \quad (3.30)$$

**Foot structure** The bottom plate of the foot, the sagittal structure and the ankle axis will be considered together for the stress analysis. The forces will be transferred from one to another and it would be harder to investigate them separately. The ankle axis will be made of a steel alloy rather than aluminium, the standard steel material from the Inventor database is taken for

this (Yield strength = 207 MPa). The forces acting on the foot bottom can be derived from the ground reaction force vector diagram that has been introduced before. This diagram shows the forces acting on the ground. We also know that these forces act at the back end of the prosthesis in the beginning of the stance and at the front end at the end of the stance.

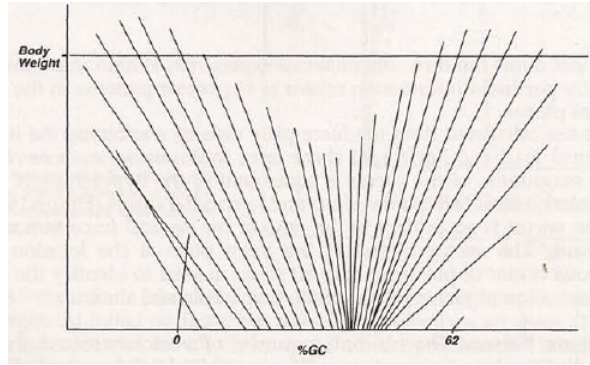


Figure 3.40: Ground reaction force vector diagram. See the chapter about biomechanics for more explanation.

Not all of these forces will be inserted in the Inventor simulation, but some load cases will be applied, representing the highest acting loads. These will be the loads at IC and at TO, when the forces act on the most extreme points of the prosthesis but only about 60% of the body weight is applied, the highest points in the force vector diagram, where about 120% of the body weight is applied. For a person of 75 kg, the body weight will be 750 N. The forces will not only be acting on the foot bottom plate but also on the ankle axis.

Other loads that are working on these parts are the forces on the ball screw bearings and the pulleys, and the force that the lever arms exert on the axis. These forces depend on how much the spring that is connected to the ball screw is elongated. The maximum value of this force is 2600 N. This force would induce a high amount of stress in the foot bottom plate if the pulleys would be attached there. To avoid this, the pulleys are connected to the sagittal structure of the foot and the connection plate is made large enough so that the forces are spread out over a larger area. The forces exerted by the lever arms are different before and after unlocking. When a lever arm is locked, a torque load is applied on the axis since the rotation is stopped by the locking mechanism. At the same time, the force that is applied on the lever arm by the springs is also applied on the axis, causing bending of the axis. When unlocked, there is no torque on

the axis and also the force causing bending will be small. The maximum torque applying is 200 Nm, just before unlocking, and the maximum force on the axis can be calculated from the positions of the lever arms just before unlocking. The calculation for the forces on the small lever is explained in Fig. 3.41, the forces on the large lever will be small compared to this force since the forces exerted by the ball screw will always be accompanied with a force in the opposite direction exerted by the small lever.

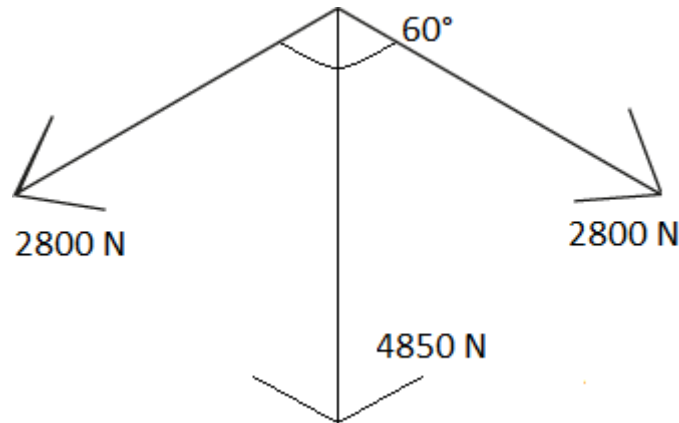


Figure 3.41: Force on the prosthesis axis due to the small lever. The two vectors of 2800 N are the forces due to the spring attached to the lever arm. 4850 N is the resultant force on the ankle axis.

For the analysis the ankle joint hole in the sagittal structure of the foot is set fixed. The problem with this is that the extra forces on the ankle due to the small lever arm is not included in the analysis since it is “carried” by the fixed constraint. For this reason, in a second analysis the bottom plate is constraint and the forces on the ankle joint are looked at. Ideally these are looked at together but a stress analysis always requires one part of the structure to be constraint. The forces due to the lever arm are only considered in the third load case, since they are the largest there.

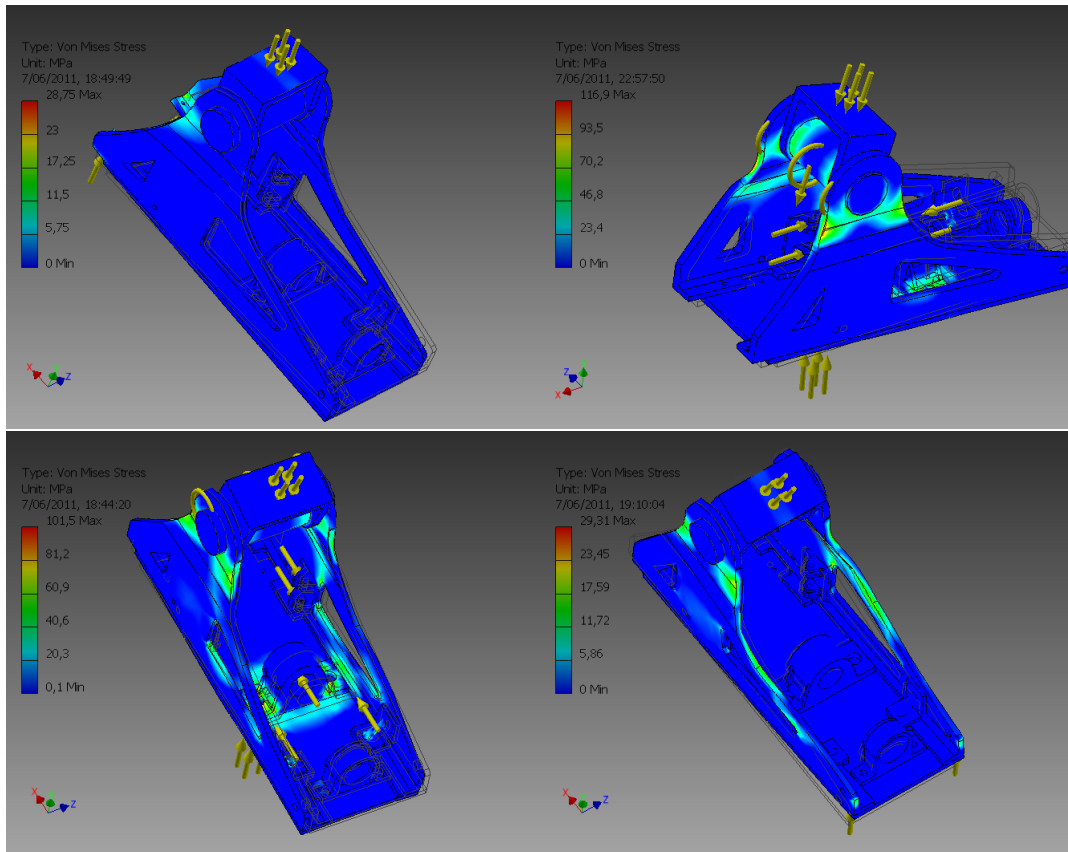


Figure 3.42: Stress in the 4 different load cases with a fixed constraint placed on the ankle hole of the sagittal structure.

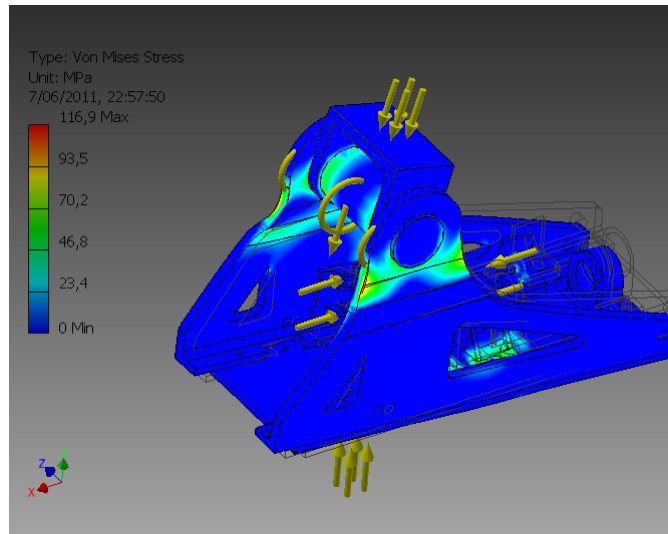


Figure 3.43: Load case 3 with a fixed constraint on the foot bottom plate.

The highest stress in all of these simulations occurs in the third load case, on the sagittal foot structure. The safety factor here is still 2.09, and combined with a dynamic bending fatigue factor this gives:

$$S = 2.09 \times 0.89 = 1.86 \quad (3.31)$$

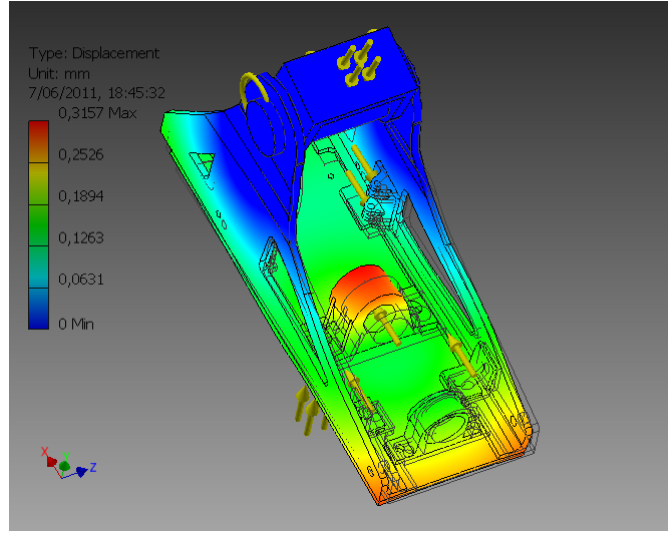


Figure 3.44: Displacement in the prosthesis for the third load case.

As can be noticed in the simulation report above, the displacement of the foot bottom plate is rather high if it is compared to the maximum radial displacement of the ball screw axis, being 0.022 mm. This can be calculated from the following formula from the ball screw data sheet:

$$e_p = \frac{l_u}{300mm} \times v_{300p} = \frac{50mm}{300mm} \times 130\mu m = 0.022mm \quad (3.32)$$

Where  $e_p$  is the permissible travel deviation, so the permissible radial displacement of one end of the ball screw compared to the other end,  $l_u$  is the useful travel length of the ball screw and  $v_{300p}$  is the permissible travel deviation within 300 mm travel, which is given in the data sheet. It is very hard to achieve a displacement of the foot bottom that is this low, the only way to do this would be to increase the thicknesses of the side structure and the bottom plate of the prosthesis. This would not be a good solution and would not lead to a compact and light design. A solution to this problem is to use a flexible coupling between the motor and the ball screw axes and use self-aligning bearings for the ball screw. This way, the displacement of the foot bottom plate is allowed to be a lot higher without obstructing the ball screw operation. For the bearing the closest to the motor, for which the axial load is the highest, a spherical plain bearing (SKF GE 8 C) is selected since these are compact and are resistant to large axial loads.

For the other bearing a self-aligning ball bearing can be used since the axial loads on this bearing will be small. Here the SKF 126 TN9 was chosen.

The flexible coupling between the motor and the ball screw would ideally be one that allows radial and angular play, but because of the lack of space a coupling that only allows angular play seems more appropriate. An example is the Belden MS20270B6.



Figure 3.45: Belden flexible transmission.

**Spring connection parts** For all of the springs, parts are designed to connect the wires to. These parts also need to withstand the forces due to the compression of the springs.



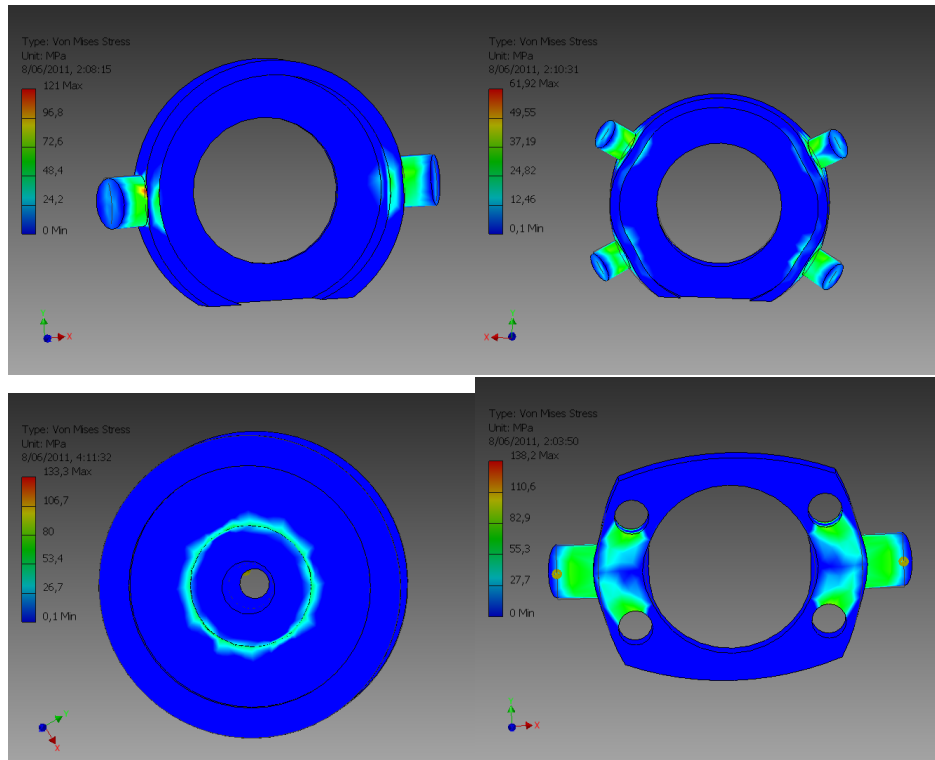


Figure 3.46: Parts made for the connection of wires to the springs and to the ball screw nut.

The minimum safety factor for these three parts is 1,99. Combined with a dynamic bending fatigue factor this gives:

$$S = 1.99 \times 0.89 = 1.77 \quad (3.33)$$

**Prosthesis mass** The mass of every part of the prosthesis can be calculated from the inventor model, other masses can be estimated or read in data sheets. The approximate masses are written down in Table 3.9.

part	weight (g)
ankle axis	270
sagittal foot structure	262
Maxon gearhead	224
2 die springs	150
ball screw with nut	120
foot bottom plate	116
Maxon motor	88
large lever arm	59
pillow blocks	46
spring connection parts	44
pulleys and spring support axis	31
torsion springs	30
small lever arm	26
toe joint and heel sensor	24
ball screw bearings	17
bolts, others (steel wire,...)	100
total	1486

Table 3.9: Overview of the approximate masses of the different components.

The total mass of the prosthesis without batteries will be well under 2 kg. This is an acceptable result when compared to the weight of other active prostheses, although the weight of passive prostheses is still significantly lower. The weight can be further reduced by using other Aluminium-alloys with higher yield strenghts like Al 7075. This material has about the same density as the used Al 6061 but a yield strenght that can be almost twice as high. This can cause the components to be designed even more compact.

## 4 General conclusions and future work

The goal of this thesis was to investigate the possibility of storing energy in one part of the gait cycle and releasing it when necessary to provide push-off. A prosthesis had to be simulated and designed that could mimick the behaviour of a sound ankle, providing enough energy to experience push-off. This energy was to be stored in a spring by a small motor during the rest of the gait cycle.

In a first stage, the human gait cycle was examined and an extensive description was made. This was important to identify the conditions the prosthesis had to meet and the tools that could be used to check the similarity between prosthesis and healthy ankle. A simulation was made to provide the data which could be used for the comparison with healthy ankle data. The simulation was also used to optimise the choice for the different components. The components that were chosen are a 30 W Maxon EC 45 flat motor, a Maxon Spur Gearhead GS 45 A with a transmission ratio of 1:32, a Bosch Rexroth ball screw mechanism with a lead of 5mm, 2 die springs with a spring constant of 200 N/mm and two small torsion springs with a spring constant of 500 Nmm/°.

A design was gradually developed in order to achieve a compact and light yet sufficiently strong prosthesis. It is capable of providing the necessary energy at the right time and above all the characteristics of the prosthesis can be fine-tuned to fit the needs of any amputee within certain boundaries. These boundaries are for example a maximum weight and maximum walking speed of the amputee, and they depend on the motor characteristics safety factors of the design. For people with a higher mass than the 75 kg that has been used for the dimensioning of the prosthesis, a driving system with a higher power is needed. A Maxon flat motor of 50 W is available which has about the same dimensions as the 30W motor that has been chosen. It should be possible to fit this motor, together with a gearbox with a smaller transmission ratio, in the prosthesis without problems.

The simulations and the design have shown that working principle of storing energy in one part of the gait cycle and releasing it in another part works and can be a good base to develop other concepts of energy storage. The drawback of this working principle is the complicated mechanical structure with the locking mechanisms and lever arms that have to be connected to

the moving springs. Passive ankle prosthesis concepts or concepts where energy from the knee joint is used to provide push-off still have to be further developed.

It is very likely that further improvements and corrections can be made to the prosthesis design. Especially when the the design of the locking mechanisms will be completed, changes will have to be made to the design. In the process of the design, it was always kept in mind that these lockings still had to be implemented, so the changes should not be extremely difficult to make, although it was not easy designing when an important part of the system was still a blackbox.

## References

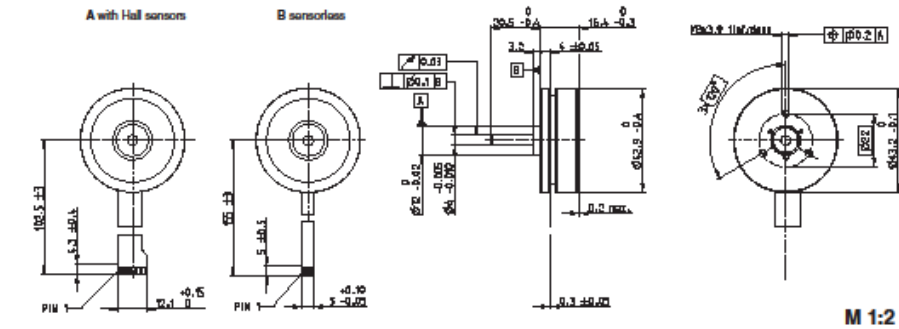
- [1] A. P. Arya, A. Lees, H. C. Nerula, and L. Klenerman. A biomechanical comparison of the sach, seattle and jaipur feet using ground reaction forces. *Prosthetics and Orthotics International*, 19(1):37–45, 1995.
- [2] S. Au, M. Berniker, and H. Herr. Powered ankle-foot prosthesis to assist level-ground and stair-descent gaits. *Neural Networks*, 21(4):654 – 666, 2008. Robotics and Neuroscience.
- [3] S. K. Au, H. Herr, J. Weber, and E. C. Martinez-Villalpando. Powered ankle-foot prosthesis for the improvement of amputee ambulation. *Conference Proceedings of the International Conference of IEEE Engineering in Medicine and Biology Society*, 2007:3020–3026, 2007.
- [4] R. Bellman, M. Holgate, and T. Sugar. Sparky 3: Design of an active robotic ankle prosthesis with two actuated degrees of freedom using regenerative kinetics. In *Proceedings of the 2nd Biennial IEEE/RAS-EMBS International Conference on Biomedical Robotics and Biomechatronics.*, 2008.
- [5] B. Brackx. Reverse engineering and redesign of a passive below-knee prosthesis prototype. Master’s thesis, Vrije Universiteit Brussel, 2010.
- [6] S. H. Collins and A. D. Kuo. Recycling energy to restore impaired ankle function during human walking. *PLoS ONE*, 5(2):e9307, 02 2010.
- [7] B. Hannaford G. K. Klute, J. M. Czerniecki. Muscle-like pneumatic actuators for below-knee prostheses. In *Actuator 2000: 7th International Conference on New Actuators*, 2000.
- [8] J. C. H. Goh, S. E. Solomonidis, W. D. Spence, and J. P. Paul. Biomechanical evaluation of sach and uniaxial feet. *Prosthetics and Orthotics International*, 8(3):147–154, 1984.
- [9] B. J. Hafner, J. E. Sanders, J. M. Czerniecki, and J. Fergason. Transtibial energy-storage-and-return prosthetic devices: a review of energy concepts and a proposed nomenclature. *Journal Of Rehabilitation Research And Development*, 39:1–11, 2002.
- [10] J. K. Hitt, R. Bellman, M. Holgate, T. G. Sugar, and K. W. Hollander. The sparky (spring ankle with regenerative kinetics) project: Design and analysis of a robotic transtibial prosthesis with regenerative kinetics. *ASME Conference Proceedings*, 2007(4806X):1587–1596, 2007.
- [11] J. Perry. *Gait Analysis: Normal and Pathological Function*. Delmar Learning, 1st edition, January 1992.
- [12] G. A. Pratt, Daniel E, Force Feedback Control Of Manipulator, Fine Motions, J. Dyn, and Syst Measurement Contr. Series elastic actuators. 1995.
- [13] J. Pratt, B. Krupp, and C. Morse. Series elastic actuators for high fidelity force control. *International Journal of Industrial Robotics*, 29(3):234–241, 2002.
- [14] A. Tehrani and M. Vermeire. Design of a below-knee prosthesis powered by electric drives. Master’s thesis, Vrije Universiteit Brussel, 2008.
- [15] W. A. R. Thomson and J. D. Comrie. *Black’s medical dictionary / by William A. R. Thomson*. Black, London :, 28th ed. edition, 1968.

- [16] G. van Oort, R. Carloni, D. J. Borgerink, and S. Stramigioli. An energy efficient knee locking mechanism for a dynamically walking robot. In *IEEE International Conference on Robotics and Automation, ICRA 2011*, USA, May 2011. IEEE Robotics and Automation Society.
- [17] R. Versluys. *Study and Development of Articulated Ankle Prostheses with Adaptable Compliance and Push-off Properties*. PhD thesis, Vrije Universiteit Brussel, 2009.
- [18] R. Versluys, A. Desomer, G. Lenaerts, O. Pareit, B. Vanderborght, G. Van der Perre, L. Peeraer, and D. Lefeber. A biomechatronical transtibial prosthesis powered by pleated pneumatic artificial muscles. *International Journal of Modelling, Identification and Control*, 4(4):394–405, 2008.
- [19] M. Whittle. *Gait analysis: an introduction*. Elsevier, 3 edition, 2002.
- [20] M. M. Williamson. Series elastic actuators. *NASA STI/Recon Technical Report N*, 96:17284–+, January 1995.
- [21] D. A. Winter. *Biomechanics and Motor Control of Human Gait: Normal, Elderly and Pathological*. Waterloo Biomechanics, 2 edition, December 1991.
- [22] J. De Witte. Mechatronic design of a soccer robot for the small-size league of robocup. Master’s thesis, Vrije Universiteit Brussel, 2010.

# Appendices

## A. Maxon EC 45 flat

### EC 45 flat Ø45 mm, brushless, 30 Watt

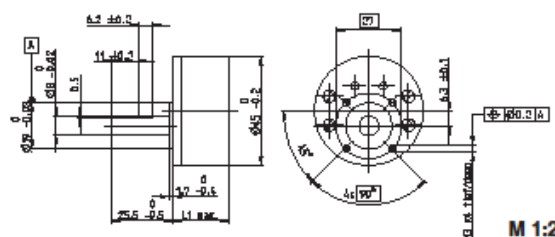


maxon flat motor

		Order Number					

### B. Maxon Spur Gearhead GS 45 A

**Spur Gearhead GS 45 A** Ø45 mm, 0.5 - 2.0 Nm



Technical Data	
Spur Gearhead	straight tooth
Output shaft	stainless steel, hardened
Bearing at output	ball bearing
Radial play, 10 mm from flange	max. 0.15 mm
Axial play	0.02 - 0.2 mm
Max. radial load, 10 mm from flange	180 N
Max. permissible axial load	60 N
Max. permissible force for press fits	60 N
Recommended input speed	< 6000 rpm
Recommended temperature range	-15 ... +80°C
Extend range as option	-40 ... +100°C

maxon gear

<input type="checkbox"/> Stock program <input type="checkbox"/> Standard program Special program (on request)		Order Number				
		301177	301175	301181	301186	301191
<b>Gearhead Data</b>						
1	Reduction	5 : 1	18 : 1	61 : 1	212 : 1	732 : 1
2	Reduction absolute	$\frac{1}{5}$	$\frac{1}{18}$	$\frac{1}{61}$	$\frac{1}{212}$	$\frac{1}{732}$
10	Mass inertia	gom <sup>2</sup> 3.7	1.6	1.0	0.8	0.8
3	Max. motor shaft diameter	mm 3	3	3	3	3
<b>Order Number</b>		<b>301178</b>	<b>301173</b>	<b>301182</b>	<b>301187</b>	<b>301192</b>
1	Reduction	7 : 1	26 : 1	80 : 1	310 : 1	1072 : 1
2	Reduction absolute	$\frac{1}{7}$	$\frac{1}{26}$	$\frac{1}{80}$	$\frac{1}{310}$	$\frac{1}{1072}$
10	Mass inertia	gom <sup>2</sup> 3.1	1.4	1.0	0.8	0.8
3	Max. motor shaft diameter	mm 3	3	3	3	3
<b>Order Number</b>		<b>301179</b>	<b>266585</b>	<b>301184</b>	<b>301188</b>	<b>301193</b>
1	Reduction	9 : 1	32 : 1	111 : 1	385 : 1	1334 : 1
2	Reduction absolute	$\frac{1}{9}$	$\frac{1}{32}$	$\frac{1}{111}$	$\frac{1}{385}$	$\frac{1}{1334}$
10	Mass inertia	gom <sup>2</sup> 2.1	1.4	0.6	0.5	0.4
3	Max. motor shaft diameter	mm 3	3	3	3	3
<b>Order Number</b>		<b>301180</b>	<b>301171</b>	<b>301185</b>	<b>301189</b>	<b>301194</b>
1	Reduction	14 : 1	47 : 1	163 : 1	564 : 1	1952 : 1
2	Reduction absolute	$\frac{1}{14}$	$\frac{1}{47}$	$\frac{1}{163}$	$\frac{1}{564}$	$\frac{1}{1952}$
10	Mass inertia	gom <sup>2</sup> 2.2	0.9	0.5	0.5	0.4
3	Max. motor shaft diameter	mm 3	3	3	3	3
4	Number of stages	2	3	4	5	6
5	Max. continuous torque	Nm 0.5	2.0	2.0	2.0	2.0
6	Intermittently permissible torque at gear output	Nm 0.75	2.5	2.5	2.5	2.5
12	Series of rotation, drive to output	" "	" "	" "	" "	" "
7	Max. efficiency	% 87	76	66	59	53
8	Weight	g 224	224	255	287	313
9	Average backlash no load	" 1.6	2.0	2.4	2.8	3.2
11	Gearhead length L *	mm 23.5	23.5	26.9	30.4	33.8



maxon Modular System								
+ Motor	Page	+ Sensor/Brake	Page	Overall length [mm] = Motor length + gearhead length + (sensor / brake) + assembly parts				
EC 45 flat, 30 W	193			40.5	40.5	43.9	47.4	50.8
EC 45 flat, 50 W	194			45.4	45.4	48.8	52.3	55.7
EC 45 flat, IE, IP 00	195			59.7	59.7		66.6	70.0
EC 45 flat, IE, IP 40	195			61.9	61.9	65.3	68.8	72.2
EC 45 flat, IE, IP 00	196			64.7	64.7	68.1	71.6	75.0
EC 45 flat, IE, IP 40	196			66.9	66.9	70.3	73.8	77.2



# C. Bosch Rexroth Miniature Nut and screw

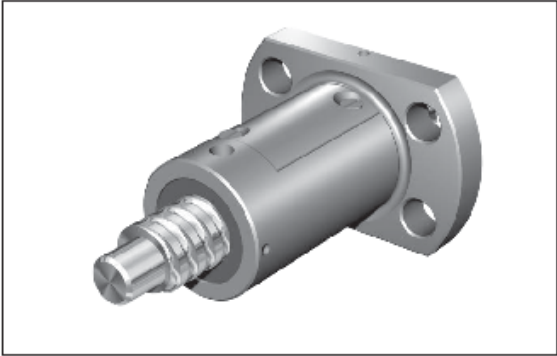
## Nuts

### Miniature Single Nut with Flange FEM-E-B

**Miniature series**  
Rexroth mounting dimensions  
Flange type B

With seals  
With backlash or reduced backlash  
For precision-rolled screws SN-R  
of tolerance grade T0, T7

Supplied only as complete ball screw  
assembly.



Ordering code: FEM-E-B 6 x 2R x 0.8-4 1 1 T7 R 83K060 41K050 250 0 1

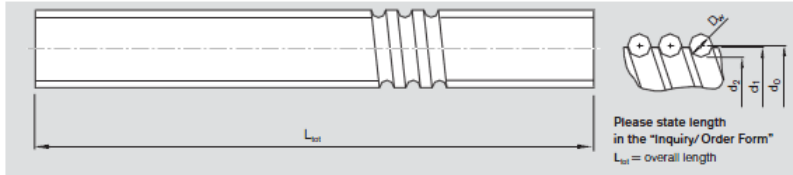
$d_0$  = nominal diameter  
 $P$  = lead  
(R = right-hand, L = left-hand)  
 $D_w$  = ball diameter  
 $i$  = number of ball track turns

Category	Size $d_0 \times P \times D_w - i$	Part number	Load ratings		Linear speed <sup>1)</sup> $v_{\max}$ (m/min)
			dyn. C (N)	stat. C <sub>0</sub> (N)	
A	6 x 1R x 0.8 - 4	R1532 100 06	900	1290	3
A	6 x 2R x 0.8 - 4	R1532 120 06	890	1280	6
A	8 x 1R x 0.8 - 4	R1532 200 06	1020	1740	3
A	8 x 2R x 1.2 - 4	R1532 220 06	1870	2760	6
B	8 x 2.5R x 1.588 - 3	R1532 230 06	2200	2800	15
B	12 x 2R x 1.2 - 4	R1532 420 06	2240	4180	12
A	12 x 5R x 2 - 3	R1532 480 06	3800	5800	30
B	12 x 10R x 2 - 2	R1532 490 06	2500	3600	60

1) See page 115 Characteristic speed  $d_0 \cdot n$  and page 150 Critical speed  $n_c$

## Screws

## Precision-Rolled Screw SN-R



Ordering code: SN 20 x 5R x 3 X X T7 R 00T200 00T200 1250 1 0

Size $d_o \times P \times D_w$	Part number Tolerance grade T5	Tolerance grade T7	Tolerance grade T9	Dimensions (mm)		Moment of inertia $J_y$ (kgcm <sup>2</sup> /m)	Maximum length (mm)		Weight (kg/m)
				$d_1$	$d_2$		Standard	On request auf Anfrage	
6 x 1R x 0.8	R1031 100 00	R1031 107 00	R1031 109 00	6.0	5.3	0.02			0.19
6 x 2R x 0.8	R1031 125 00	R1031 127 00	R1031 129 00	6.0	5.3	0.02			0.19
8 x 1R x 0.8	R1031 205 00	R1031 207 00	R1031 209 00	8.0	7.3	0.04			0.36
8 x 2R x 1.2	R1031 225 00	R1031 227 00	R1031 229 00	8.0	7.0	0.04			0.36
8 x 2.5R x 1.588	R1031 235 00	R1031 237 00	R1031 239 00	7.5	6.3	0.04			0.30
12 x 2R x 1.2	R1031 425 00	R1031 427 00	R1031 429 00	11.7	10.8	0.13	1500	2500	0.79
12 x 5R x 2	R1031 465 10	R1031 467 10	R1031 469 10	11.4	9.9	0.11			0.75
12 x 10R x 2	R1031 495 00	R1031 497 00	R1031 499 00	11.4	9.9	0.11			0.74
16 x 5L x 3	R1051 015 00	R1051 017 00	R1051 019 00	15.0	12.9	0.31			1.24
16 x 5R x 3	R1011 015 00	R1011 017 00	R1011 019 00	15.0	12.9	0.31			1.24
16 x 10R x 3	R1011 045 00	R1011 047 00	R1011 049 00	15.0	12.9	0.31			1.23
16 x 16R x 3	R1011 065 10	R1011 067 10	R1011 069 10	15.0	12.9	0.34			1.29
20 x 5R x 3	R1011 115 00	R1011 117 00	R1011 119 00	19.0	16.9	0.84			2.03
20 x 5L x 3	R1051 115 00	R1051 117 00	R1051 119 00	19.0	16.9	0.84			2.03
20 x 10R x 3	R1011 145 00	R1011 147 00	R1011 149 00	19.0	16.9	0.84			2.03
20 x 40R x 3.5-4	R2021 150 00	R2021 170 00	R2021 190 00	19.0	16.4	0.86			2.06